

Modelling of wind energy conversion system

BACHELOR THESIS



GRADO EN INGENIERÍA EN TECNOLOGÍAS INDUSTRIALES

POLITECHNIKA WARSZAWSKA

WARSAW UNIVERSITY OF TECHNOLOGY

FACULTY OF ELECTRICAL ENGINEERING

AUGUST, 2020

AUTHOR: ALEXIS ANSELMO GÓMEZ GÓMEZ

DIRECTOR: Dr hab. inż. Grzegorz Iwański





TITLE		Modelling of wind energy conversion system	
AUTHOR		Alexis Anselmo Gómez Gómez	
SUPERVISOR		Grzegorz Iwański	
DEGREE	Grado en ingeniería en tecnologías industriales	DATE	06/08/2020

Keywords

Wind power, Wind energy, energy conversion, inverter, boost converter, voc.

Objective of the thesis

The main objective of this thesis is the modelling of a wind energy conversion system composed by the wind turbine and all the necessary equipment to connect it to the grid in order to supply power to this one.

Description of the thesis

In the first place the problem is divided into all the different components that are a part of the final model, this is done for two main reasons, the first one being to work in an easier way by dividing the main model into smaller and simpler ones, the second one is that due to differences of speed of operation between the various components, it is easier and faster to simulate their behaviour in separate ways.

For the wind turbine it will be used the model from the computer software PSIM, that later will be exposed.

The electrical machine of choosing, to generate electrical energy from the mechanical energy provided by the wind turbine, is a permanent magnet synchronous machine, which the model is also in the PSIM library.

Then the rectifier and DC switching converters, used to transform the alternating current signal provided by the previous electric machine (generator) to a direct current one. After that, the DC wave is treated with a boost converter. The model for these two components will be developed.

After the DC is treated, it goes through an inverter, which transforms it back to an AC wave, with optimum power factor, and its connected to the grid.

As it is seen the main focus of this thesis are the power electronics components and its control, using several techniques to try that the electrical machine and the wind turbine are working with optimum efficiency.



Index

Keywords.....	3
Objective of the thesis	3
Description of the thesis	3
Summary	6
Resumen.....	6
Specifications	7
Wind turbine	7
Electrical machine (PMSM)	7
Boost converter.....	7
Inverter.....	7
Grid.....	7
The project	8
Introduction to wind power	8
History	9
Current wind turbines	12
Current conversion systems.....	14
The model	15
Wind turbine	15
Generator	19
DC switching converter	22
Boost converter	23
Averaged boost converter.....	24
MPPT	25
Inverter.....	28
Averaged inverter.....	31
Complete model.....	33
Averaged complete model	34
Simulations and results	35
Steady state.....	35
Transitory regime	38
MPPT	39
Tip-speed ratio	39
Optimum torque	41



Power signal feedback..... 42

Conclusions 43

References..... 44

Annex 1: Table of illustrations..... 46

Annex 2: Transformation and inverse transformation from *abc* to *dq* space. 48

Annex 3: Transformation from *abc* to *alpha-beta* ($\alpha\beta$) space. 49



Summary

For the completion of this project, a complete model of a wind energy conversion system (*Back to back*) connected to the grid has been made, which some of the sub-models conforming it have been done by third parties, whereas others have been made specifically for this project.

It has been considered an installation of 20 kW of power, using a permanent magnet synchronous machine, given the amount of power to transmit, we face a three-phase machine.

Both the wind turbine and the electric machine models can be found in the PSIM library, nevertheless later on they will be described.

To treat the power generated by this electrical machine a diode rectifier, a boost switching converter and an inverter, connected to the grid, are used to dump the power into this last one. Also, an optimum power factor is required and some MPPT strategies will be exposed.

Finally an adequate system is obtained with PFC and a THD bellow 5%, which makes the system grid compatible, moreover, this is done by multiple simple control strategies (MPPT and open loop) and a basic topology.

Resumen

Para la realización de este proyecto se ha llevado a cabo el modelado completo de un sistema de energía eólica system (*Back to back*) conectado a la red, para parte del modelo global se han utilizado modelos previamente realizados por terceros y modelos desarrollados específicamente para este.

Se ha tenido en cuenta una instalación de 20 kW de potencia con una máquina eléctrica síncrona de imanes permanentes, dada la potencia a transmitir, nos encontramos ante una máquina trifásica.

Tanto el modelo de la turbina eólica como de la máquina eléctrica se encuentran en la librería de PSIM, aunque serán descritos más adelante.

Para el tratamiento de la energía generada por esta máquina eléctrica se utilizan un rectificador de diodos; un convertidor, basado en conmutación, elevador y un inversor que se encontrará conectado a la red, a la que volcará la potencia. También se requiere un factor de potencia óptimo y se muestran diferentes estrategias para MPPT o "*Maximum power point tracking*".

Finalmente se llegará a un sistema adecuado con regulación del factor de potencia y una distorsión armónica menor del 5%, lo que permite su acoplamiento a la red, que además es logrado mediante varias estrategias de control (MPPT y lazo abierto) y una topología simples.

Specifications

Wind turbine

Magnitude	Value
Nominal output power	20 kW
Base wind speed	15 m/s
Base rotational speed	100 rpm
Moment of Inertia	8000 kg m ²

Electrical machine (PMSM)

Magnitude	Value
Stator Resistance	18 mΩ
Self-inductance coefficient (Direct axis)	175 μH
Self-inductance coefficient (Quadrature axis)	180 μH
Voltage peak to peak / krpm	244.94
Number of poles	20
Moment of Inertia	42.1 · 10 ⁻³ kg m ²
Shaft time constant	10

Boost converter

Magnitude	Value
Self-inductance coefficient	5 mH

Inverter

Magnitude	Value
Input capacitor	1 mF
Self-inductance coefficient 1 (L ₁)	2 mH
Self-inductance coefficient 2 (L ₂)	2 mH
Capacity	20 μF

Grid

Magnitude	Value
Voltage (Line to line, RMS)	400 V
Frequency	50 Hz

The project

Introduction to wind power

Wind energy is a renewable and clean source of energy that is based on the wind's kinetic energy. Wind can be defined as a mass of air in movement as a result of the difference in atmospheric pressure, generally caused by a heterogeneous distribution of solar radiation that generates a gradient in temperatures.

Eolic power plants generate electric energy from the wind using wind turbines, however there are wind speed and flow fluctuations during the operation of these devices, which results into a signal of complicated treatment and many negative repercussions on the network if not properly corrected. Also given the unpredictability of the resource, power plants with high regulation characteristics and fast response are necessary, so if one Eolic park stops producing another power central can generate the power previously supplied by the park.

From an environmental perspective its impact on nature is relatively small, mainly:

- Acoustic pollution during operation.
- Distorting the landscape.
- Endangering the birds and bats around several kilometres.

Even though only around 2% of all solar power that reaches Earth (Lastra, 2015) is actually transformed into wind power, and on top of this only a fraction of this is usable, estimations put the potential at around 20 times of the world's total energy consumption; which makes wind power one of the most important sources of energy, not only as a renewable source, but in general.

For all of this, besides being a mature enough technology, the market share and participation in the energy mix of several systems has been growing at increasing rates. For example, the growth for wind energy in the European Union from 2011 to 2014 was 9.6 %, whereas from 2014 to 2017 it was of 15 %.

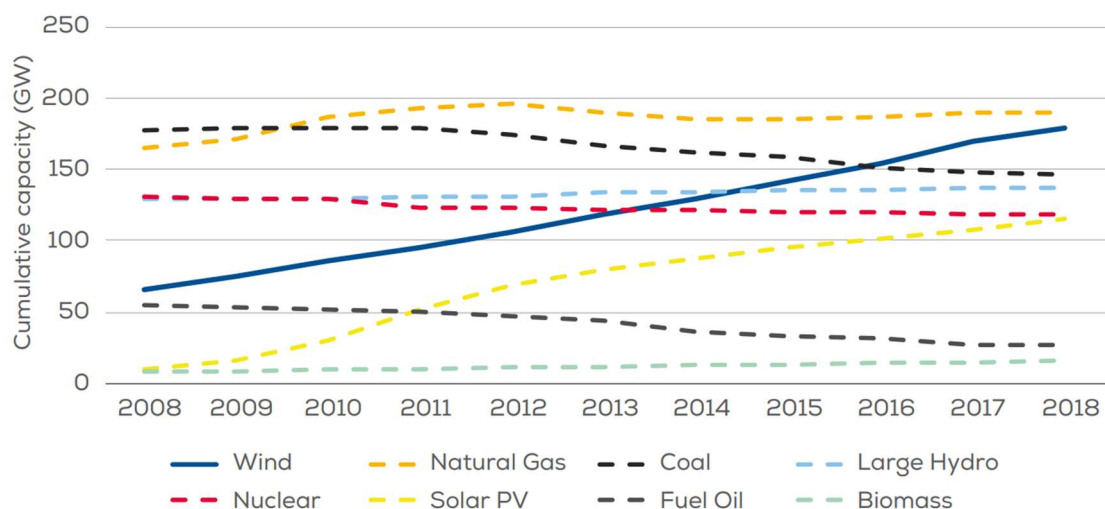


Figure 1: Total power generation capacity in the European Union 2008-2018. Source: (WindEurope, 2019).

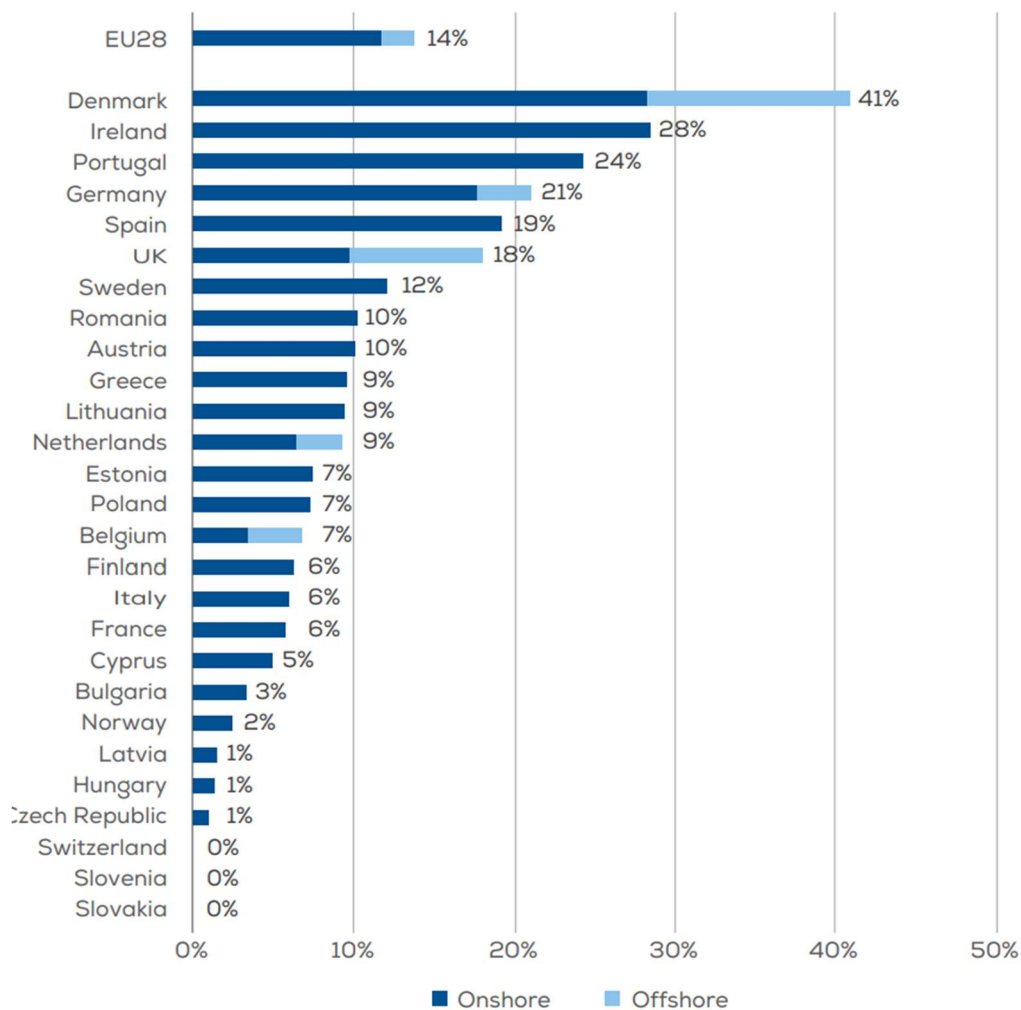


Figure 2: Percentage of the average annual electricity demand covered by wind¹. Source: (WindEurope, 2019).

History

Harnessing the wind was one of the first challenges of the human kind, harnessing a force of nature itself to use in the benefit of those who managed to do it, creating endless possibilities that were not doable before like sailing, pumping water or milling grain in a scale never seen before with less effort, those are some of the examples of the earliest accomplishments in this field that go as far as China during the second century B.C. Those machines were built with rudimentary and common materials with a vertical axis.

During the XIII century the first horizontal axis wind turbines appeared in Europe for the same uses as the previous ones, although these new models had better efficiency. These were very popular and very quickly generalized, especially in England and Holland, influencing other cultures.

¹ The figures represent the average of the share of wind in final electricity demand, captured hourly from ENTSO-E and corrected thanks to national TSOs and BEIS data. Data is not available from all European countries.



Figure 3: Windmills, Campo de Criptana, Spain. Credit: Lourdes Cardenal.

During the XIX century and later the so called “Western-wheel” expanded rapidly, mostly in the USA. These are composed by several (18 to 20 generally) sheets of steel arranged in fan positions. By the end of the 1930s more than 8 million units had been installed, the most common scenario was water pumping, which represents a key factor for the colonization of the American Wild West. With the invention and development at the end of the XIX century the first Eolic generators were based in already existing designs of wind turbines. The first person to create a wind power generator in the sense that we today understand was Charles F. Brush in 1888. In Denmark Professor Poul Lacour developed a mil capable of reaching the 25 kW mark with a turbine diameter of 25 m.

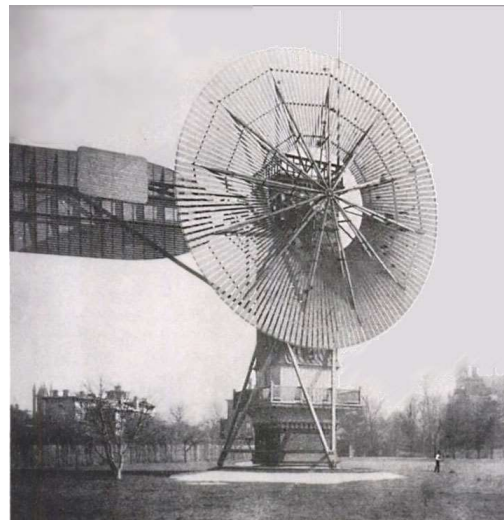


Figure 4-. Charles F. Brush's turbine. Ohio, 1888.

Next, throughout the XX century the aerodynamic theory suffered a series of advancement mainly caused by the efforts of Germany, Russia and France. Among these discoveries the one made by German Betz, that says that the greater the rotational speed the more efficient the turbine is and that it is limited at 60 %, was extremely interesting.

After WWI, the generalization of electric energy and the complex political situations, facilitated the development of this technology at all scales of production. This trend was followed until the

WWII, after which due to the intense use of oil-based technologies and the lack of capabilities to predict correctly the wind, the research almost stopped. Years later, during the first oil crisis the development and popularity of this mean of production was reignited in an effort to make this technology more attractive, environmentally and economically (wind turbines were quite expensive), and reduce the influence of the countries in control of oil. For this to happen different governments, especially European, gave grants for installation and research of new installations. This trend was continued during the 80s and Eolic power gained traction as an alternative to have in mind, and was continued by some countries to this day.

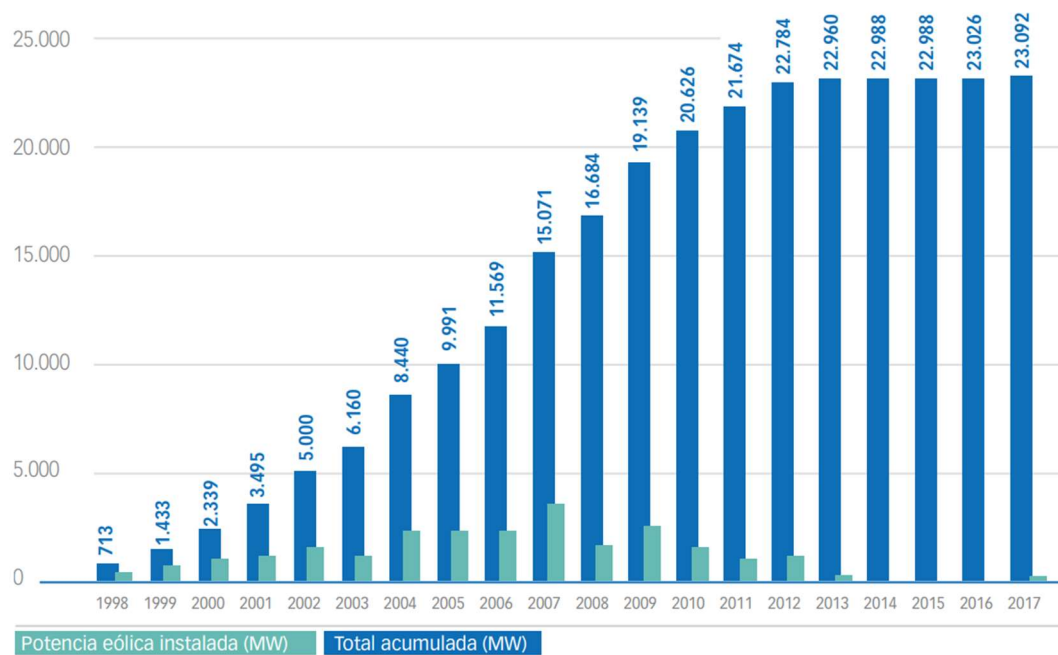


Figure 5: Annual evolution and accumulated power in Spain. Green: Installed wind power (MW), Blue: Accumulated power. Source: (Asociación Empresarial Eólica, 2018).



Current wind turbines

A wind turbine can be defined as a machine that converts the power in the wind into electricity, contrary to a windmill, as this machine does not transform the mechanical energy of the wind into any other type.

Wind turbines can be classified according to different criteria, some of the more common ones are:

- Place of installation
 - Onshore: This type of turbine is installed on land. These are the more common due to their greater simplicity.
 - Offshore: This type of turbine is installed on water (sea). They have higher cost of maintenance and reduced accessibility. On the other hand, the availability of wind is greater than in their counterparts, being almost constant within the same period of time; finally, in some countries because of topography or due to an already developed wind power system, can be hard to find adequate sites on land. For these reasons this type of turbines are gaining traction and more countries are betting on them.
- Power output
 - Micro: From Watts to a few kW. They are designed for personal use to decrease the energy consumption (from the grid).
 - Mini: There is no strict classification but they can be considered installations up to 100 kW, and with only one turbine. They are used to supply electricity to isolated areas, to complement certain industries and factories or for grid supply.
 - Normal: More than 100 kW or one turbine.
- Axis orientation
 - Vertical: The characteristic of this wind turbine is that the main axis is perpendicular to the ground, making possible that no matter the direction of the wind it can be used, therefore it does not need orientation mechanisms. The gearbox, generator, converters and other necessary devices are situated at ground level, facilitating the maintenance. Their main setback is the worse efficiency and performance than those of horizontal axis.
 - Horizontal: The axis is parallel to the ground; therefore, it needs an orientation system, either passive or active (for bigger turbines), all the devices necessary for correct operation are situated at the top, which makes maintenance more expensive and complicated; however, this type enjoys a greater efficiency.
 - Number of blades: 2, 3 (most common for high power) or multiblade.
 - Rotor configuration can be upwind or downwind.
 - Power control: Aerodynamic control or variable pitch control.
 - Transmission of mechanical power: Direct or indirect.

As it was previously pointed out the most common turbines are the horizontal axis ones or HAWT, reaching some of the more modern and greater powers of several MW, especially for offshore models.

The main parts of a HAWT are:

- **Rotor:** The rotor is formed by the blades and the hub, these are two of the key parts in terms of cost, efficiency and performance. The blades suffer the force enforced by the wind and transmit it to the hub, modern blades can be around 30 m in length. The hub ties together all the blades and the shaft, generally at the slow speed side.
- **Drive train:** It is composed by all rotating components, these typically include the low-speed shaft, the high-speed shaft, bearings, couplers, a brake (Mechanical emergency brake) and a gearbox. The gearbox allows to transform the rotational speed from the hub side to the generator side to a suitable level of rotational speed, some thousands of rpms. For turbines of high power special and more robust design is necessary to transmit all the power, making the components bigger and heavier. It is necessary to have in mind the special dynamic components of wind turbines.
- **Generator:** It is the electrical machine in charge of transforming the mechanical energy transmitted by the high-speed shaft into electrical energy. Several types can be used but the more common ones are induction and synchronous generators, for lower powers a PMSM (Permanent magnet synchronous machine) can be used. If the connection is direct, the rotational speed of the shaft is related with the electrical frequency of the network and the number of poles of the machine. This approach reduces enormously the speed margin and induces more stress on the turbine. Other alternative is to generate electric energy trying to maintain the system at the maximum point of power and then treat the power adequately, this can be done by use of power electronics.
- **Nacelle and yaw system:** This set contains the cover, the main frame and the yaw system. The cover protects the contents from the weather, the main frame serves as a point to fix and align the drive train. The yaw system maintains perpendicular the wind direction with the plane of the blades.
- **Tower and foundation:** The tower is usually made of steel tubes, lattice or concrete with a height generally of 1 to 1.5 times the diameter of the rotor, but at least 20 m. During the design stage it is very important to consider resonance effects, vibrations and noise provoked by the wind, the weather or the wind turbine itself (tower shadow²).
- **Controls:** A set of sensors, computers, power circuit components and mechanical actuators that control and regulates the behaviour of the turbine.
- **Other components necessary for power management.**

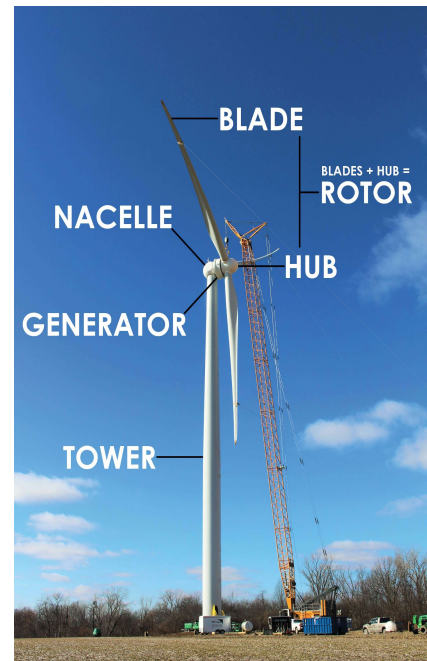


Figure 6: Diagram graphically depicting parts of a wind turbine, including the tower, generator, nacelle, blade, hub, and rotor. Source: (One Energy Enterprises LLC, 2020)

² The effect of tower shadow produces a periodic decrease in mechanical torque due to the passing of one of the blades in front of the tower, that changes the airflow. This is produced with frequency 3 times the rotational frequency for a tri-blade turbine.

Current conversion systems

- **Fixed Speed:** This type of conversion system is characterized by the fixed rotational speed of the generator, set by the frequency of the grid, as this one is directly connected to the output. As the frequency is set, the efficiency of this type of systems is reduced if compared with those of variable speed. The only variable that can be controlled is the reactive power consumption if provided with some extra equipment. Under this category we find both, synchronous and asynchronous machines.
- **Variable speed:** This type is characterized by the presence of power electronics that allows the generator to run at variable rotational speeds depending on the configuration of the system. There are several strategies such as: Coupling all generators to a DC grid using rectifiers, using a thyristor or PWM (pulse-width modulation) converters to transform AC-DC-AC (Back to back), a Double-fed asynchronous generator, in which only part of the generated power goes through the power electronics or a combination of several systems with different types of electrical machines. All in all, this category of conversion systems usually is more efficient and therefore used. In this case a Back to back scheme is exploited.

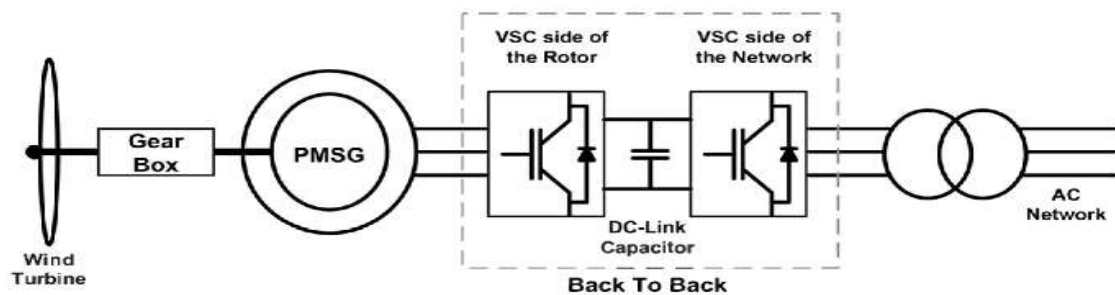


Figure 7: General scheme of a wind power back to back conversion system. Source: (N. M. Salgado-Herrera, 2015)

The model

As it was previously discussed, the complete model was divided into different smaller ones during the development phase.

Wind turbine

This model was separated for several reasons, it is the only purely mechanical element in the model and the reaction and operational speed of it is much slower than the rest of the components, therefore it requires of much longer simulation times. By creating a separate model, we reduce greatly the amount of time destined for simulation.

For this part of the project, the included “Wind turbine” model in PSIM software was used. This was done as the main focus of the complete model is the power conversion not the mechanical or electricity generation parts.

This model is constructed over the equation of power generated by a wind turbine (Heier, 2014):

$$P = \frac{1}{2} \cdot A \cdot v_{wind}^3 \cdot \rho \cdot C_p$$

Where:

- A is the area covered by the blades.
- v_{wind} is the relative speed between the air and the turbine, in our case the wind speed.
- ρ is the density of the air ($\rho_{air} \approx 1.225 \text{ kg/m}^3$).
- C_p is the coefficient of power.

$$C_p = C_1 \cdot (C_2 - C_3\beta - C_4\beta^x - C_5) \cdot e^{-C_6} + C_7$$

Where:

- β is the pitch angle of the blades in degrees.
- x is a modification factor, generally $x=2$.

C_1	C_2	C_3	C_4	C_5	C_6	C_7
0.5	$116 \cdot \lambda'$	0.4	0	5	$21 \cdot \lambda'$	$0.01 \cdot \lambda$

- λ is the tip speed ratio: $\lambda = \frac{\omega_m \cdot R_{blade}}{v_{wind}}$
 - ω_m is the rotational speed of the blades in rad/s.
 - R_{blade} is the radius of the blade in m.

$$\lambda' = \frac{1}{\lambda + 0.08} - \frac{0.035}{\beta^3 + 1}$$

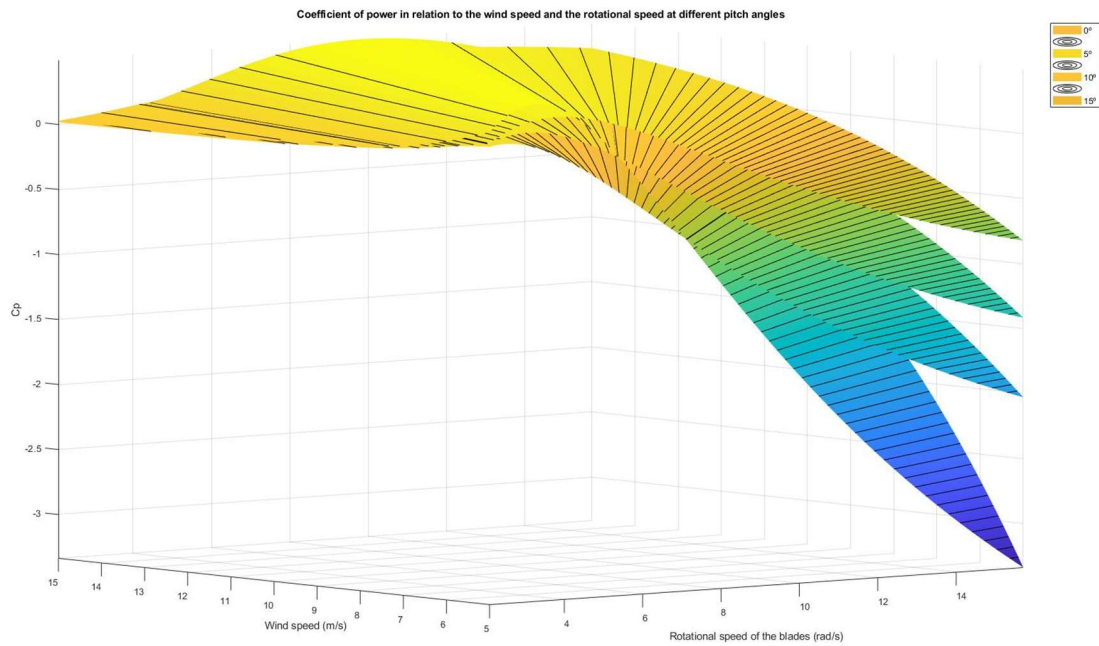


Figure 8: Power coefficient in relation to the wind speed and rotational speed at different pitch angles ($R=12.5$ m, $x=2$)

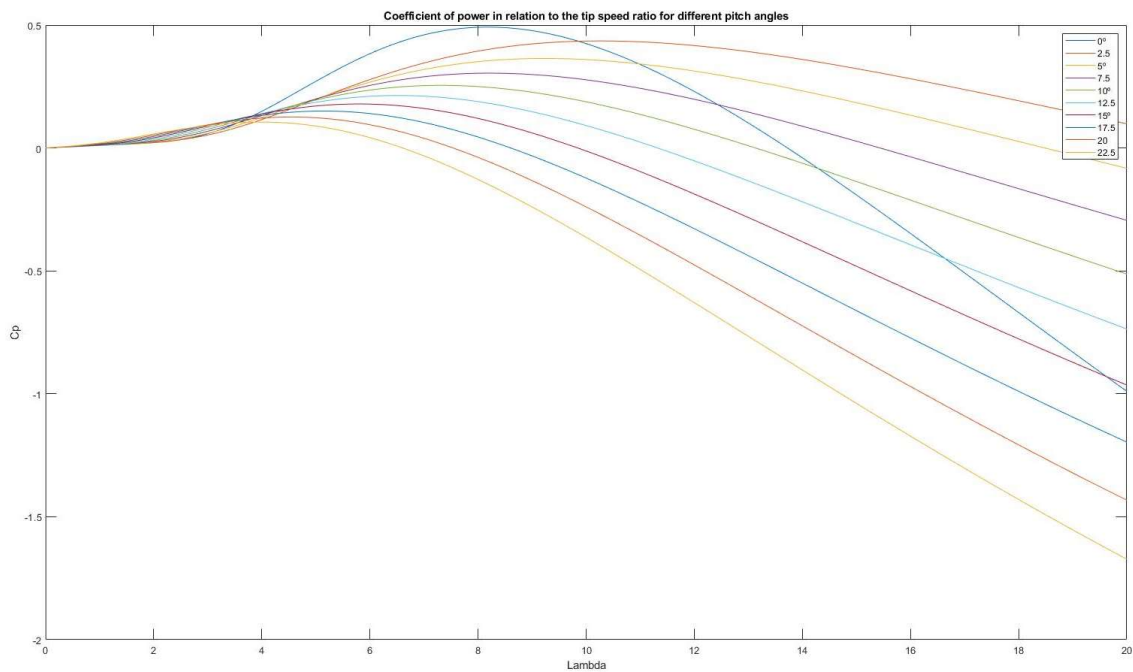


Figure 9: Power coefficient in relation to tip speed ratio for different pitch angles ($R=12.5$ m, $x=2$)

Of this model, a control strategy can be derived, to maintain the turbine at the point where maximum power is extracted from the wind. Using a simple PSIM model, with the wind turbine block, different constant wind speeds and supposing pitch angle equal to 0° , connected to a mechanical load; it is possible to obtain different curves describing the characteristic of our own wind turbine.

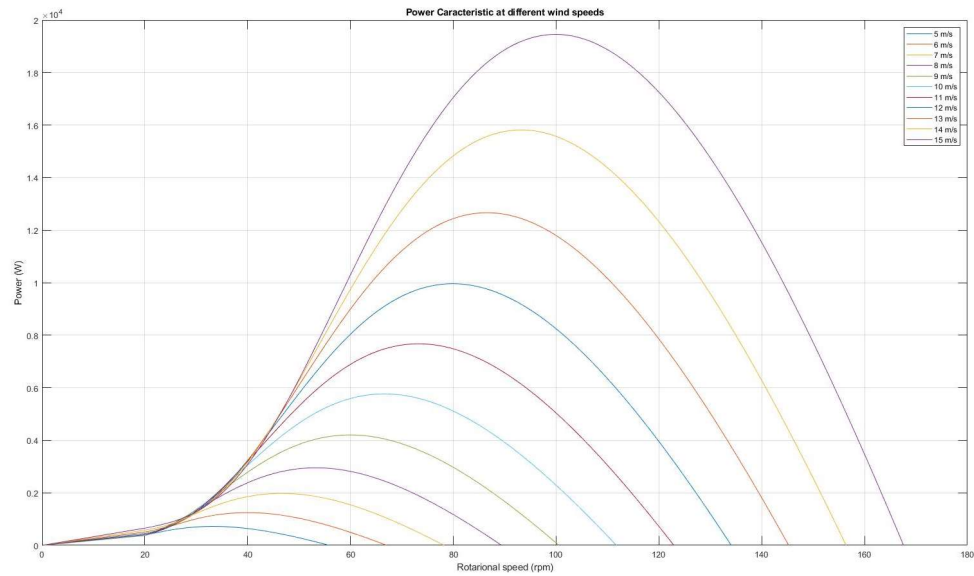


Figure 10: Power characteristic at different wind speeds

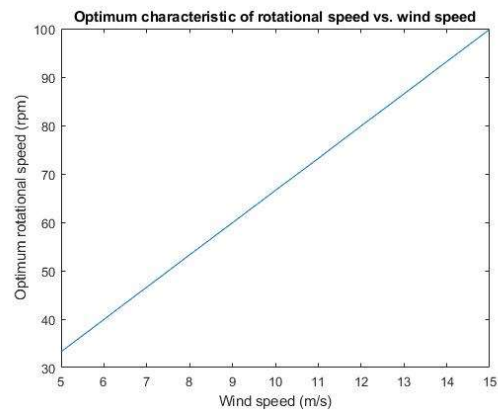


Figure 11: Optimum characteristics of rotational speed vs. wind speed

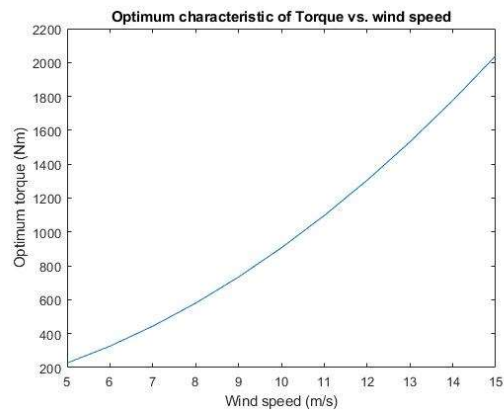


Figure 12: Optimum characteristic of torque vs. wind speed

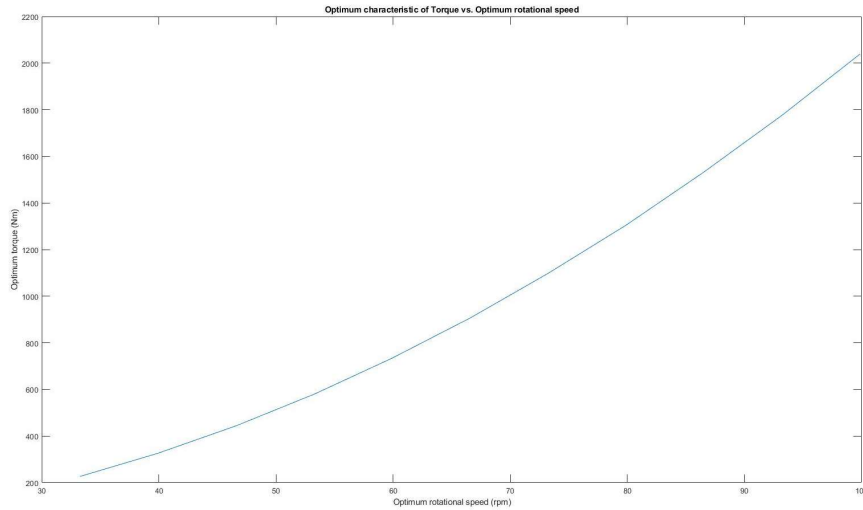


Figure 13: Optimum torque vs. optimum rotational speed

Using this data it is possible to extrapolate an equation that maintains the wind turbine giving the optimum torque according to the actual rotational speed. By using this analytical method, it is not necessary a torque sensor.

$$T = 0.205 \cdot n^2$$

Where n is the actual rotational speed in rpm.

For the power limitation, we choose to use the pitch angle of the blades in relation to the direction of the wind, to find an appropriate equation that is able to control this variable, an analysis of the wind turbine at different wind speeds and different pitch angles was done. From this analysis, an approximated cubic polynomial equation was extracted.

$$v = (\text{wind speed} - \text{base wind speed})$$

$$\text{pitch} = 0.003574 \cdot v^3 - 0.1864 \cdot v^2 + 4.159 \cdot v - 3.003$$

It is due to denote that, as it can be seen in the figure, the result is then limited on the lower side by 0.

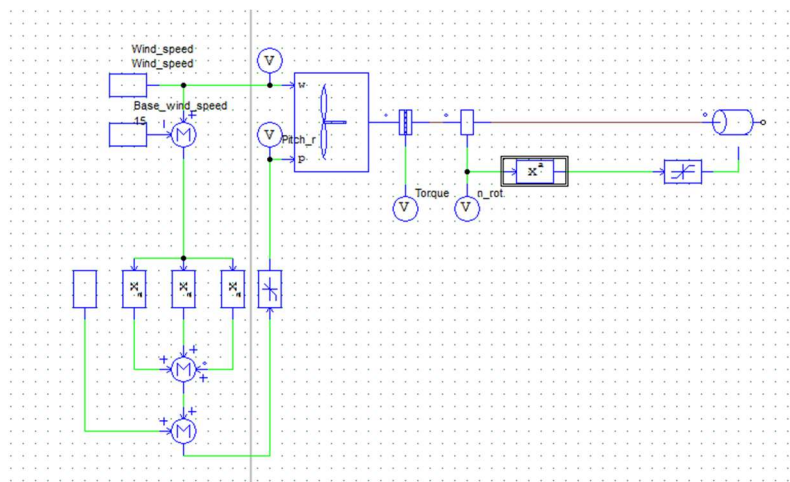


Figure 14: Schematic of the mechanical model

Generator

For the generator a permanent (Blanco Rubio, 2017) magnet synchronous machine has been chosen for several reasons. The use of this type of machines was greatly influenced by the evolution of the field of permanent magnets; which are materials that with no natural magnetic field of their own, once magnetised the magnetic field formed in them is highly persistent.

A traditional synchronous machine is composed by three fundamental parts: The stator, the rotor and the gap between them. The stator is constructed of staked plates made of a magnetic material, such as an alloy of iron and silicon, and it has one or multiple AC multi-phase winding. The rotor is made of a ferromagnetic material, such as iron alloys, and a DC winding which generates a constant magnetic field, and this winding can be replaced by a permanent magnet.



Figure 15: Small permanent magnet synchronous machine. Source: Water Fuel Energy Solutions.

The adjective synchronous is applied to these machines because they spin at the synchronous frequency, established by the frequency of the power supply and the number of poles.

$$n = \frac{60 \cdot f}{p}$$

Where:

- n is the synchronous rotational speed in rpm.
- f is the supply system frequency in Hz.
- p is the number of pairs of poles.

This type of machines (PM) can be divided into two according to the electrical power supplied:

- DC brushless motors, are fed by a DC current which thank to a switching-based inverter is able to actuate the shaft. However, this is a very simple control strategy that generates a considerable torque ripple, and it is generally used at lower powers.
- AC brushless motors, more commonly denominated PMSM, are fed by an AC current, which reduces the aforementioned torque ripple, increases the field density in the gap and improves the performance.

There are several main advantages and disadvantages associated, such as:

- Advantages
 - No field inductor on the rotor, avoiding copper losses and improving performance.
 - No need for bushes or slip rings, therefore simpler maintenance.
 - For both of the previous reasons, the machine is more compact and simpler, increasing the power density, the torque and improving the dynamic response.
- Disadvantages
 - The generated magnetic field cannot be regulated and only modified by weakening strategies.
 - More complex control.

The model used in the project is the one included in the PSIM library, which follows these equations (Powersim Inc, 2018):

$$\begin{bmatrix} v_a \\ v_b \\ v_c \end{bmatrix} = \begin{bmatrix} R_s & 0 & 0 \\ 0 & R_s & 0 \\ 0 & 0 & R_s \end{bmatrix} \cdot \begin{bmatrix} i_a \\ i_b \\ i_c \end{bmatrix} + \frac{d}{dt} \begin{bmatrix} \lambda_a \\ \lambda_b \\ \lambda_c \end{bmatrix}$$

Where:

- v_a, v_b and v_c are the stator phase voltages.
- i_a, i_b and i_c are the stator phase currents.
- λ_a, λ_b and λ_c are the stator phase flux linkages.
- R_s is the stator phase resistance.

The flux linkages are defined as:

$$\begin{bmatrix} \lambda_a \\ \lambda_b \\ \lambda_c \end{bmatrix} = \begin{bmatrix} L_{aa} & L_{ab} & L_{ac} \\ L_{ba} & L_{bb} & L_{bc} \\ L_{ca} & L_{cb} & L_{cc} \end{bmatrix} \cdot \begin{bmatrix} i_a \\ i_b \\ i_c \end{bmatrix} + \lambda_{pm} \begin{bmatrix} \cos(\theta_r) \\ \cos(\theta_r - \frac{2\pi}{3}) \\ \cos(\theta_r + \frac{2\pi}{3}) \end{bmatrix}$$

Where:

- θ_r is the rotor electrical angle³.
- λ_{pm} is the peak stator phase flux linkage:

$$\lambda_{pm} = \frac{60 \cdot V_{pk/krpm}}{\sqrt{3} \cdot \pi \cdot P \cdot 1000}$$

- P is the number of poles.

³ Magnetic or electric angle is a concept used in electrical machines. This represents an angle having into account the number of poles in the machine, this is done this way as it is considered that when some element is aligned with the north pole, south pole and then north pole again, the cycle is completed. Or in other words:

$$\text{Magnetic angle} = \frac{\text{Geometric angle}}{p}, \text{ where } p \text{ is the number of pairs of poles.}$$

The stator inductances (self and mutual) are defined as:

$$L_{aa} = L_s + L_o + L_2 \cdot \cos(2\theta_r)$$

$$L_{bb} = L_s + L_o + L_2 \cdot \cos(2\theta_r + \frac{2\pi}{3})$$

$$L_{cc} = L_s + L_o + L_2 \cdot \cos(2\theta_r - \frac{2\pi}{3})$$

$$L_{ab} = L_{ba} = -\frac{L_o}{2} + L_2 \cdot \cos(2\theta_r - \frac{2\pi}{3})$$

$$L_{ac} = L_{ca} = -\frac{L_o}{2} + L_2 \cdot \cos(2\theta_r + \frac{2\pi}{3})$$

$$L_{bc} = L_{cb} = -\frac{L_o}{2} + L_2 \cdot \cos(2\theta_r)$$

Where:

- L_s is the stator leakage inductance.

If we apply the transformation from the abc space to the dq frame we obtain much simpler equations:

$$L_d = L_s + \frac{3}{2}L_o + \frac{3}{2}L_2$$

$$L_q = L_s + \frac{3}{2}L_o - \frac{3}{2}L_2$$

In this frame the torque is:

$$T_{em} = \frac{3}{2} \cdot p \cdot (\lambda_{pm} \cdot i_q + (L_d - L_q) \cdot i_d \cdot i_q)$$

Where p is the number of pair of poles.

The torque produced by the wind turbine is transferred to the shaft of the generator through an ideal gearbox with a gear ratio⁴ 20. This is done so the rotational speed in the generator side is greater, thus making possible the generation of electric energy at a higher voltage.

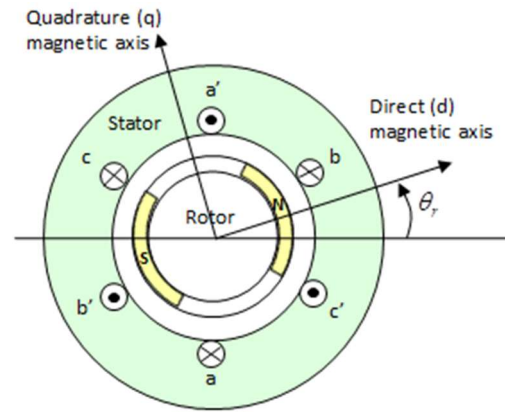


Figure 16: Diagram of a PMSM. Source: The MathWorks, Inc.

⁴

$$\text{Gear ratio}^{-1} = \frac{\omega_{input}}{\omega_{output}} = \frac{1}{20} \rightarrow \text{due to conservation of power} \rightarrow \frac{T_{output}}{T_{input}}$$

DC switching converter

The 3-phase current generated by the generator is not suitable for grid connection, that is why this is converted to DC, treated and then back to AC for dumping the power into the network.

In order to convert the AC to DC a diode rectifier is used, this has been chosen instead of an active rectifier as there is no need for bi-directional flow of power and the waves are going to be modified. This is a simpler alternative that does not require any control, which simplifies the model; however, the output ripple and potential energy losses are greater.

After the current has been rectified, a boost converter rises up the voltage, this device is current controlled, so that the current through the inductor of the switching converter is the adequate amount for the generator to require the torque at which the wind turbine operates under optimum efficiency.

For this to happen the converter operates in a closed loop in which the reference current is derived, with a series of conversions factors, from the actual rotational speed of the shaft on the wind turbine side, from which we obtained the reference torque for this part. The factors are the one from the gearbox and the constants from the electrical machine and the rectifier, it is due to note that the equation as such is not just a multiplying factor, but it has been approximated as one. The error signal is regulated by a PI controller, scaled and compared against a symmetrical triangular signal with frequency 10 kHz to obtain the PWM signal for the MOSFET transistor. Again, as the bi-directional flow of power is not needed the other ideal switch is realized by a simple diode.

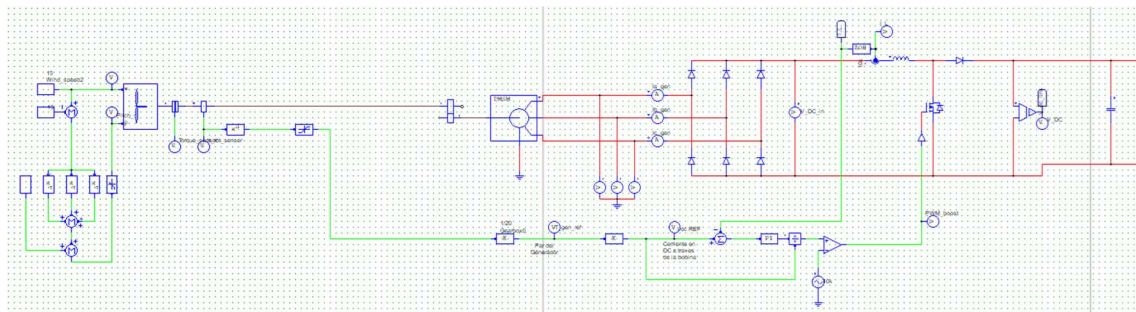


Figure 17: Schematic of the wind turbine, generator, rectifier and boost converter.

Coefficient	Value
Gearbox (Power circuit)	0.05
Generator and rectifier (Control circuit)	0.445
PI Gain	0.2
PI time constant	0.01
Self-inductance coefficient of the inductor	5 mH

In order to maintain adequate simulation times for the previous schematic the boost converter can be replaced by his averaged version, which by using we lose some information, but the general behaviour of the model is the same.

Boost converter

The boost converter model follows a series of equations for steady state based (CCM)⁵ on the inductor volt-second balance, capacitor charge balance and the small ripple approximation.

$$\begin{aligned} \langle v_L \rangle_T &= V_g \cdot D + (V_g - V_{out}) \cdot (1 - D) = 0 \\ \langle i_C \rangle_T &= -\frac{V_{out}}{R} \cdot D + \left(i_L - \frac{V_{out}}{R}\right) \cdot (1 - D) = 0 \end{aligned}$$

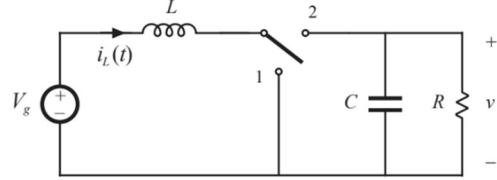


Figure 18: Schematic of a Boost converter.

Source: (Erickson & Maksimović, 2001)

Where:

- $\langle v_L \rangle_T$ is the average value of the voltage of the inductor.
- V_g is the input voltage.
- V_{out} is the output voltage.
- D is the duty cycle.
- $\langle i_C \rangle_T$ is the average value of the current through the capacitor.

By solving these two equations and assuming a low ripple in the current through the inductor we obtain the relation between the output and input voltage, as well as the DC current component through the inductor:

$$V_{out} = \frac{V_g}{1-D} \quad I_L = \frac{V_{out}}{(1-D) \cdot R}$$

For the calculation of the ripple of the current:

$$\frac{di_L(t)}{dt} = \frac{v_L(t)}{L}$$

Considering a linear behaviour:

$$\Delta I_L = \frac{V_g}{2L} \cdot D \cdot T_s = \frac{V_g - V_{out}}{2L} \cdot (1 - D) \cdot T_s$$

For the capacitor:

$$\Delta V_C = \frac{V_{out}}{2RC} \cdot D \cdot T_s$$

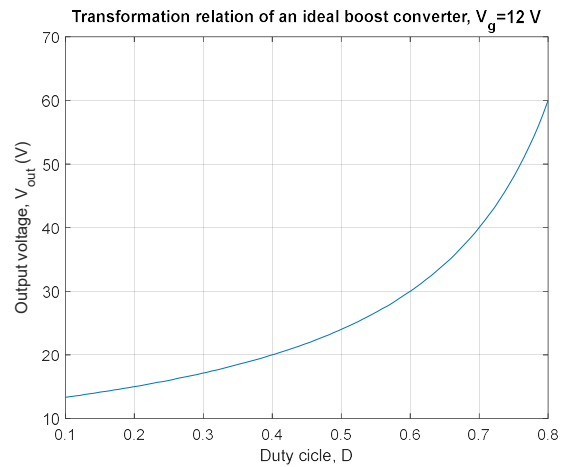


Figure 19: Transformation ratio of an ideal Boost converter.

From these two last equations given the specifications of the converter, the capacity and the coefficient of self-inductance can be calculated. So, in summary, this converter allows us to give an output voltage greater than the input voltage.

⁵ CCM or Continuous Conduction Mode is the mode in which the boost converter operates as long as the ripple of the inductor is smaller than the average value of the current through it, making the instantaneous inductor current never equal to 0. If this happened the converter would operate in Discontinuous Conduction Mode or DCM, changing its behaviour and rendering this model not valid.

MPPT

The maximum power that can be extracted from an energy source, especially renewable, not only depends on the “available power” of the source but also in the point the system operates. MPPT stands for Maximum Power Point Tracking, which is a fundamental concept for increasing performance, this concept has been used in different algorithms and techniques for wind power conversion systems.

All of the implemented and evaluated algorithms for this model are categorized as “Lookup table based”, it must be said that there are modifications and variations of these that are not discussed, as they are based in the characteristics of the controlled system, contrary to other algorithms. These have several particular and general disadvantages, such as:

- Air density: All these methods use data calculated with a model that supposes a constant air density, that may be different to the one where and when the systems operates.
- Aging factors: With the course of time, some of the components, especially mechanical, deteriorates and change the maximum efficiency and the point at which it is reached.
- Non constant efficiencies: All of these methods focus on reaching the MPP for the wind turbine, therefore maximizing the mechanical power. However, the objective is to produce electrical power, which depends in several components. And it may be the case that the MPP for the wind turbine is not actually the MPP for the entire system.

Tip-speed Ratio

The tip-speed ratio is a constant coefficient given by the wind turbine; this coefficient relates the tip speed with the wind speed. If the optimum ratio is maintained the system is bound to work at the MPP. This optimum point is obtained experimentally.

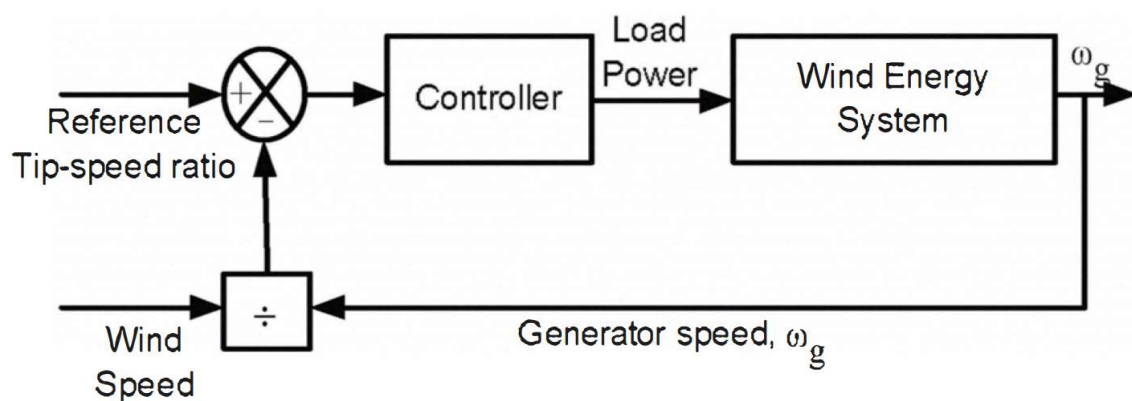


Figure 23: Block diagram of the tip speed ratio control. Source: (M. A. Abdullah, 2011)

This approach requires a very precise instantaneous measurement of the wind speed, which can be relatively complex.

Optimum torque

This method is based in a reference torque derived from the wind turbine power and the tip-speed ratio:

$$P = \frac{1}{2} \cdot A \cdot v_{wind}^3 \cdot \rho \cdot C_p \quad v_{wind} = \frac{w_m \cdot R}{\lambda}$$

And combining both equations:

$$P_m = \frac{1}{2} \rho \pi R^5 \frac{\omega_m^3}{\lambda^3} C_p$$

Where:

- A is the area covered by the blades.
- v_{wind} is the relative speed between the air and the turbine, in our case the wind speed.
- ρ is the density of the air ($\rho_{air} \approx 1.225 \text{ kg/m}^3$).
- λ is the tip-speed ratio.
- w_m is the rotational speed.
- R is the rotor radius.
- C_p is the coefficient of power.

And by considering that the mechanical power is the product of the torque and the rotational speed,

$$T_{m-opt} = \frac{1}{2} \rho \pi R^5 \frac{C_{pmax}}{\lambda_{opt}^3} \omega_m^2 = K_{opt} \omega_m^2$$

Therefore, we obtain a torque reference to use in a feedback loop.

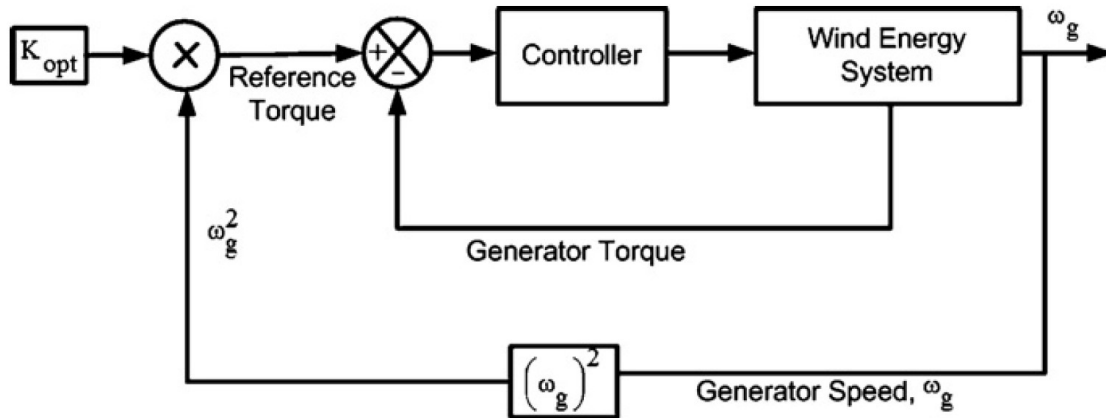


Figure 24: Block diagram of optimal torque control MPPT method. Source: (M. A. Abdullah, 2011)

For this situation, instead of using a torque sensor to obtain the generator torque it can be obtained by the electrical magnitudes, given that the torque is proportional to the current.

Power signal feedback

This technique establishes the power reference from a table, obtained from experimental results, and a rotational speed input that is used in a feedback loop and gives as an output the rotational speed.

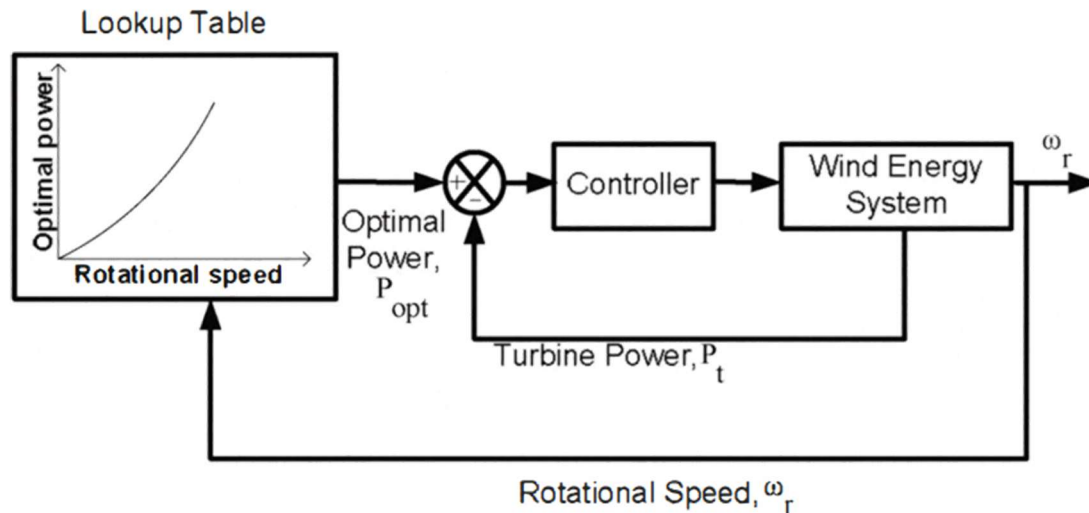


Figure 25: block diagram of a wind energy with the power signal feedback control technique. Source: (M. A. Abdullah, 2011).

However, to evaluate the power generated by the turbine, instead of using a torque sensor it can also be measured the electrical power after the generator and then the output would be the DC voltage, as it was exposed by (Wang & Chang, 2004), though this makes the “inertia” for the control loop higher.

Perturb & Observe

The perturbation and observation (P&O), or hill-climb searching (HCS) technique is a mathematical optimization technique oriented to find local maximums of a given function, making this useful for a system with only one maximum. This approach consists on changing or perturbing a control variable in small steps and observing how the systems reacts to this stimulus, getting closer to the MPP. This concept can be applied to electrical or mechanical variables. This method, as oppose to the other does not require any previous knowledge about the system to control and does not require additional sensors nor measurements, therefore making it ideal for renewable sources of energy. However, as this is an iterative process, the step size is a compromise between accuracy and faster responses; and for any case the capability of following a moderate or big and quick change in wind speed for medium to large inertia turbines is not enough, this problem is even bigger in the case that the control variables are from the electrical system, as the inertia is greater. This method is not use in the case of wind power, but it is interesting to see how is used in similar and less dynamic technologies, such as photovoltaic energy.

There are several compromises and partial solutions to some of them:

- Adaptable step size: The variable step depends on the slope of the curve between successive iterations, this way the trade-off precision vs. faster response is mitigated.
- Dual step size: It uses a smaller step size after the MPP of the larger step size has been found. Improves efficiency marginally.
- Search-remember-reuse: Turns the perturb & observe algorithm into a lookup table one.
- Modified to avoid generator stall: Adds a faster control parameter.
- Limit cycle based: Acts according to the DC link voltage.
- Disturbance based: Proposes to inject a sinusoidal perturbation instead of a step.
- Self-tuning senseless: With high peak detector capability and deriving the rotational speed from the current frequency. From this data estimates the optimal power curve.

All of these modifications that affect the P&O algorithm have advantages and disadvantages that can make this technique applicable in some cases for wind power, but as it was already warned it is not the case for large turbines.

Other techniques might include fuzzy logic, neural networks or linearization, for example.

Inverter

The power obtained from the DC link needs to be converted into AC so it can be dumped to the grid. To do this a three-phase two-level inverter architecture has been chosen for several reasons:

- Easy architecture to implement and control, only six transistors.
- Valid for low DC voltages, as each transistor withstand half the value of the DC link.
- Good enough for a slow application (50 Hz) with low dynamic requirements, that results in an acceptable total harmonic distortion.
- The power is relatively small.

Additionally, a LCL filter is implemented to reduce the wave distortion.

The control strategy is a simple voltage-oriented control (VOC), which implies that a reference DC link voltage is established as, at least 1.61 times bigger than the grid line to line voltage.

$$v_{line\ to\ line\ (max)} = \frac{\sqrt{3}}{\sqrt{2}} \cdot m_a \cdot \frac{V_{DC}}{2} \qquad \text{Modulation index} = m_a = \frac{V_{control}}{V_{carrier}}$$

(Hussain, Sher, Murtaza, & Al-Haddad, 2019)

$$\text{Modulation frequency} = m_f = \frac{f_{switching}}{f_{1^{st}harmonic}}$$

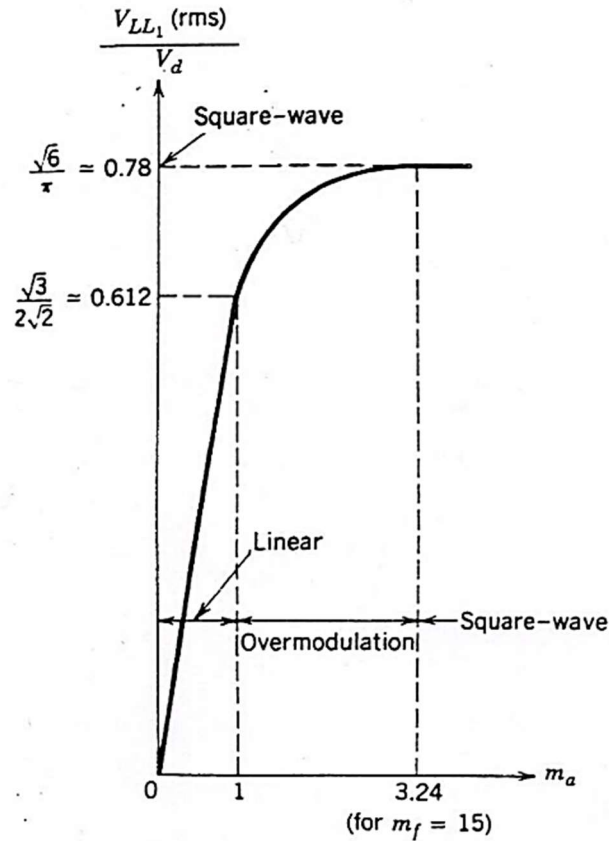


Figure 26: Line to line grid voltage in relation to the modulation ratio. $V_{DC}=350$ V, $f=60$ Hz. Source: (Kazmierkowski, Blaabjerg, & Krishnan, 2002)

Out of the linear range the sinusoid wave is not possible due to limitations in amplitude.

This strategy is realised by an outer voltage control loop that sets the reference for the I_d current of the inner control loop, responsible for the real power part of the inverter, while the I_q is set to 0, making the power factor to the grid close to 1. These two currents are compared against the phase currents in a rotating frame reference. The obtained signal from the loop is then added with the dq values of the voltage, to reduce dynamic behaviour, transformed back to abc coordinates to obtain the switching signals, again by comparison against a triangular symmetrical carrier signal. The control signal before is compared is scaled down to the level of the carrier signal to improve the results, and work with a modulation index of 1 or less.

To do both transformations is necessary to know the phase angle θ , which is obtained from the grid voltage using an abc to alpha-beta coordinates transformation and doing the inverse tangent operation with both components.

An LCL filter is added to eliminates the harmonics generated by the switching of the transistors.

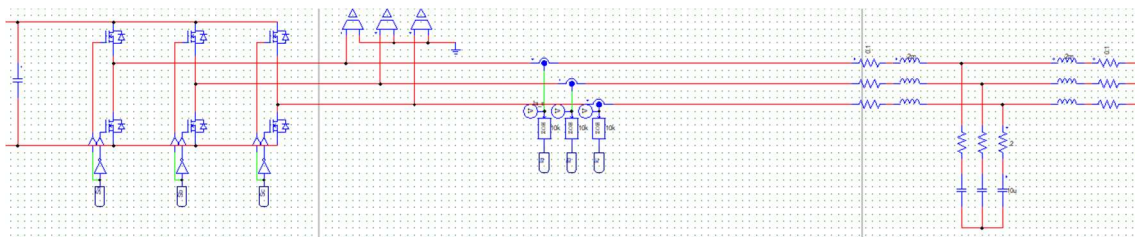


Figure 27: Inverter and LCL filter schematic.

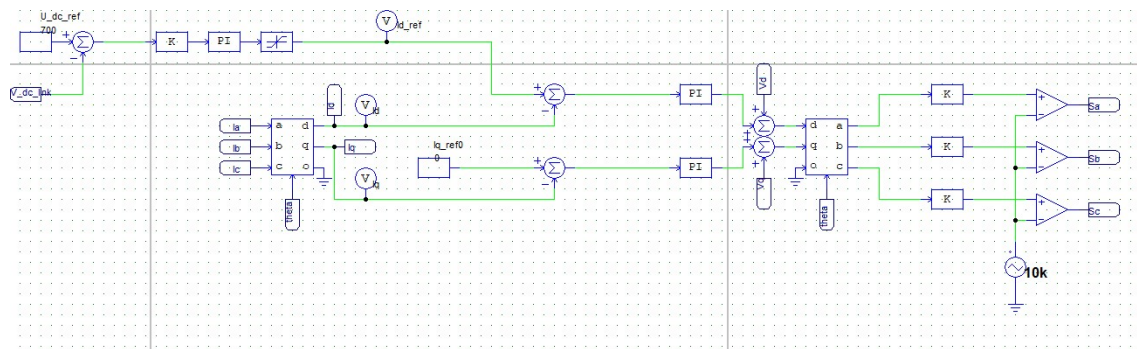


Figure 28: Inverter Voltage Oriented Control.

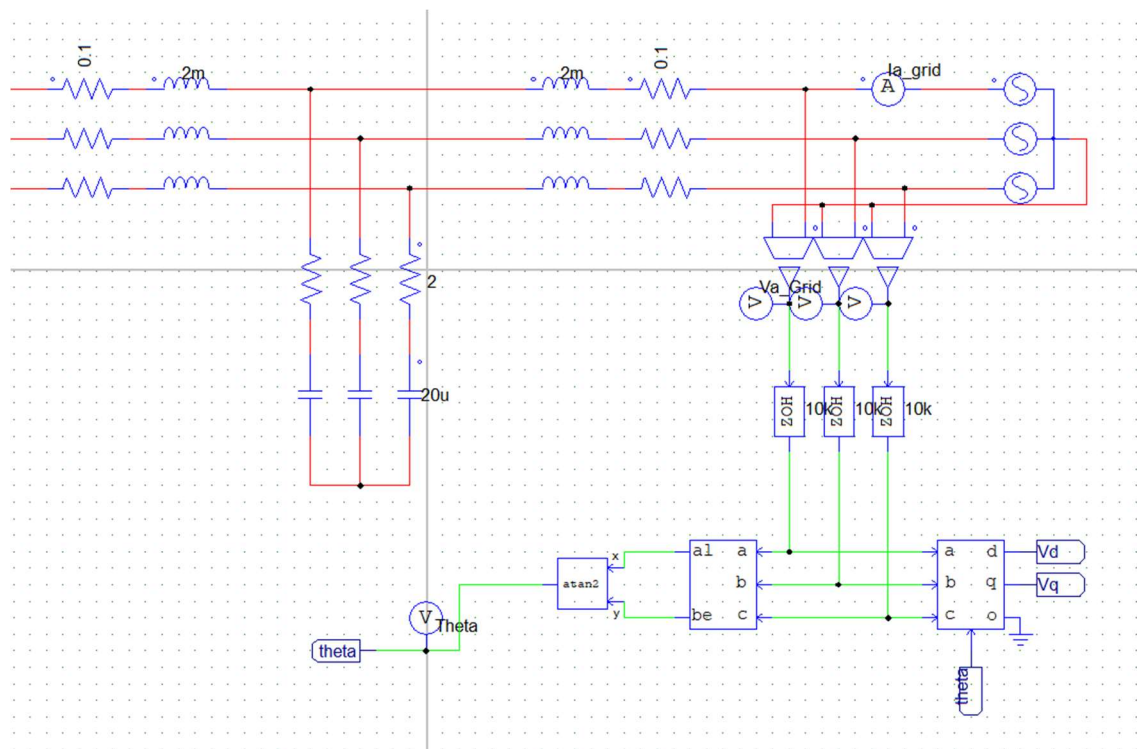


Figure 29: Calculation of theta angle for the abc to dq transformation.

Averaged inverter

For the same reasons as in the case of the boost converter an average model for the inverter is created by using voltage dependant sources, at the AC side and dependant current sources at the DC side.

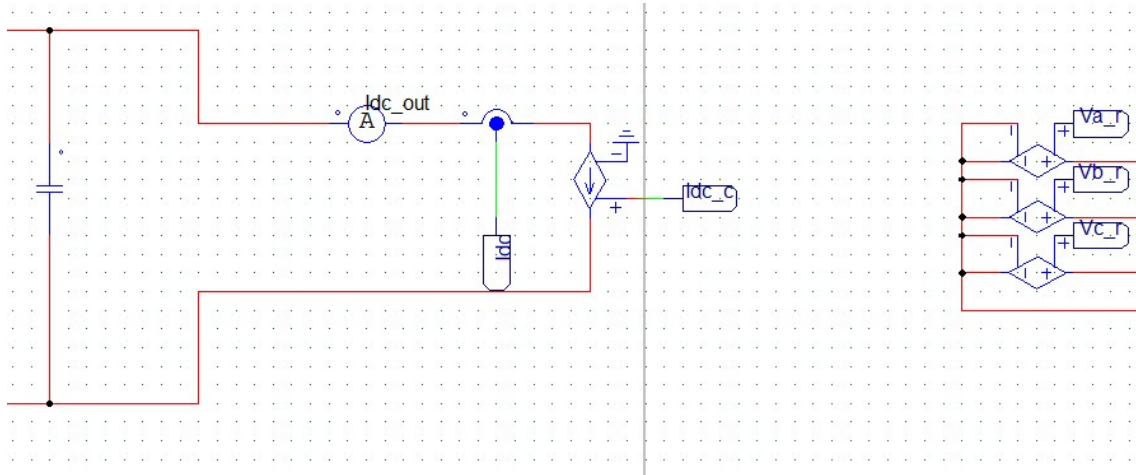


Figure 30: Averaged inverter schematic.

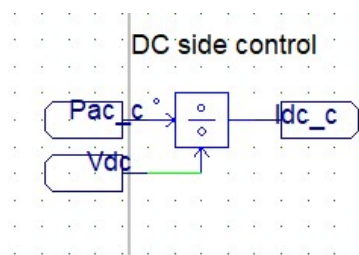


Figure 31: Averaged inverter DC side controller.

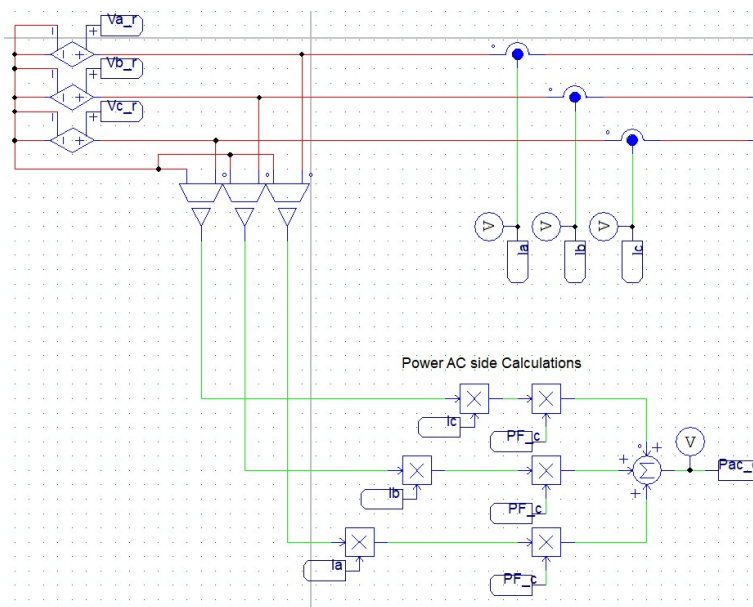


Figure 32: Calculations for consumed power at the AC side.

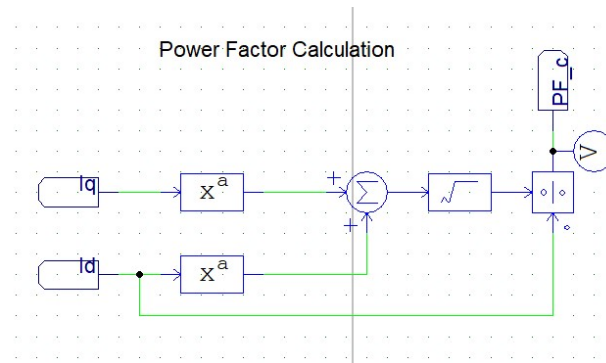


Figure 33: Power factor calculation.

For the control of the voltage dependant sources is used the same VOC approach as in the instantaneous model.

Complete model

The complete model consists in a combination of all the other models, as it was stated at the beginning.

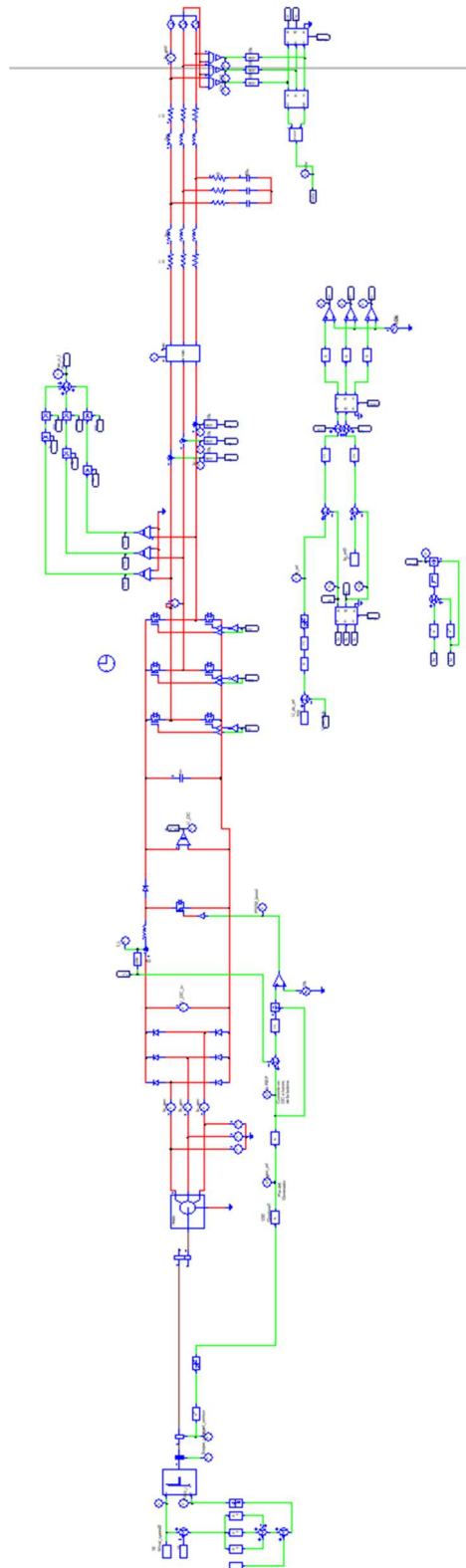


Figure 34: Complete schematic.

Averaged complete model

Again, the averaged model is also de combination of the different averaged models.

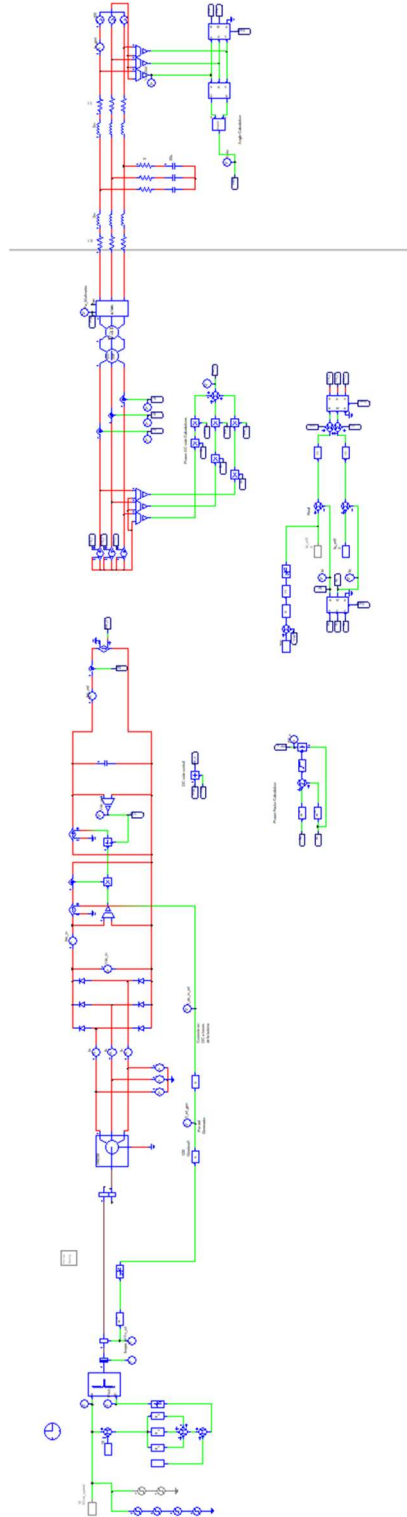


Figure 35: Complete schematic for the average model.

Simulations and results

Steady state

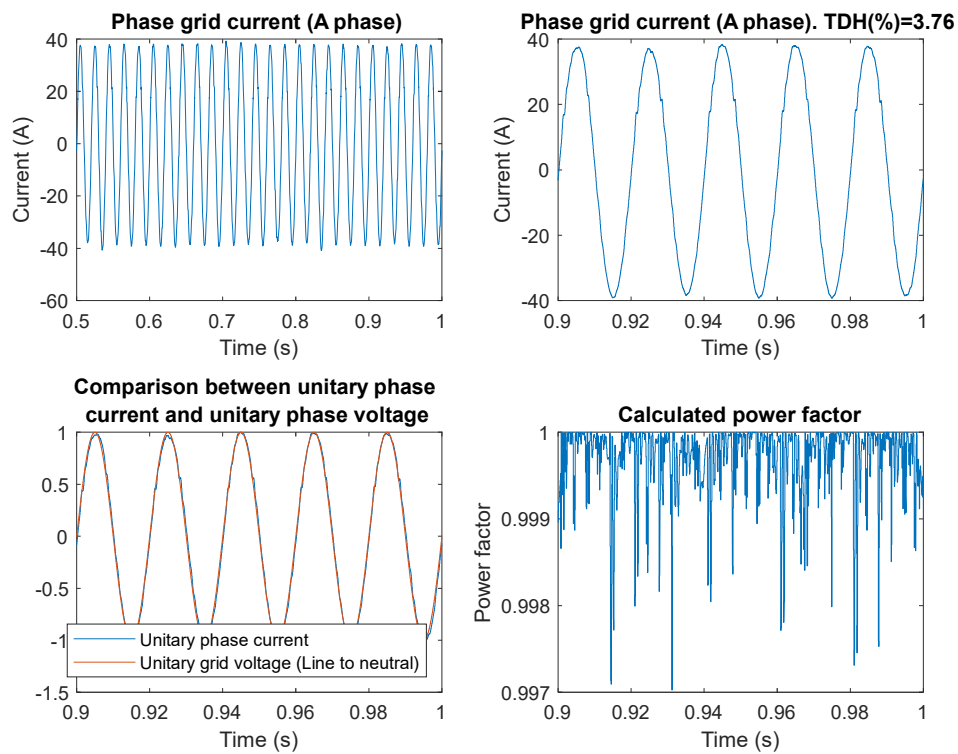


Figure 36: Steady-state "Grid-side" results.

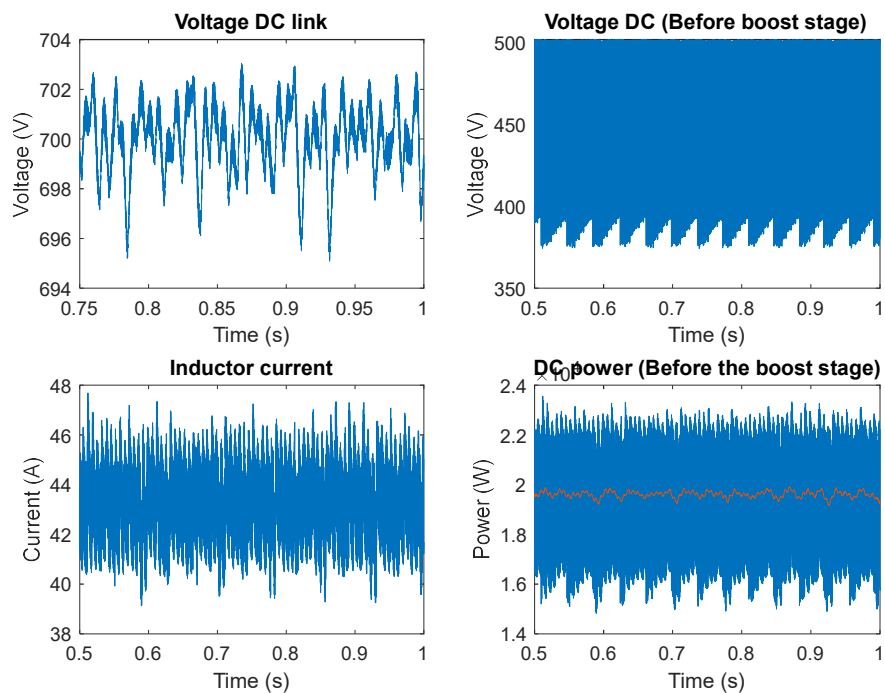


Figure 37: Steady-state DC link results.

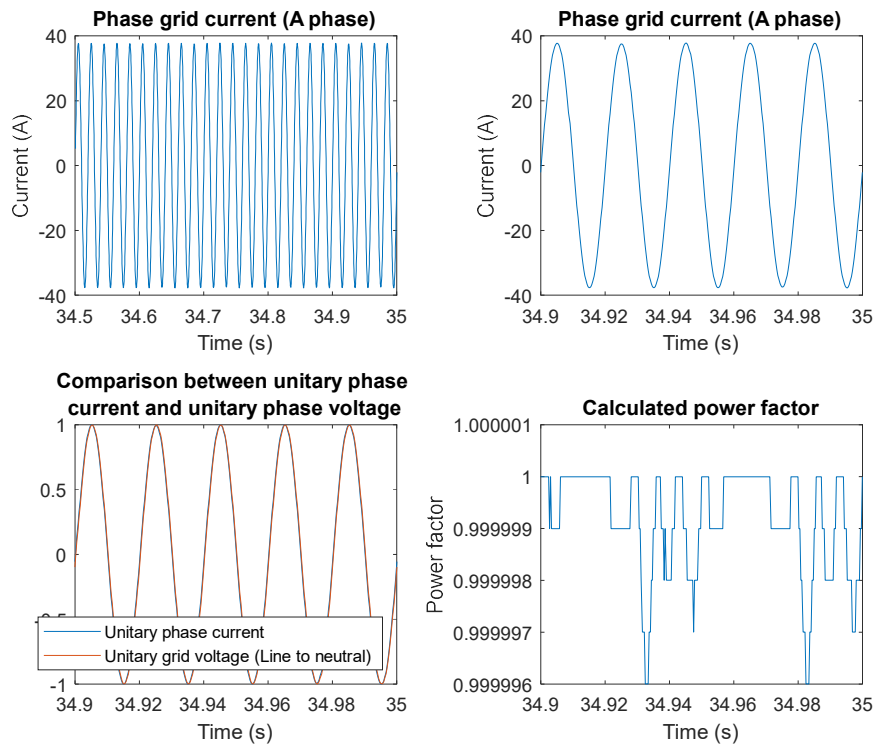


Figure 38: Steady-state average model "Grid side" results.

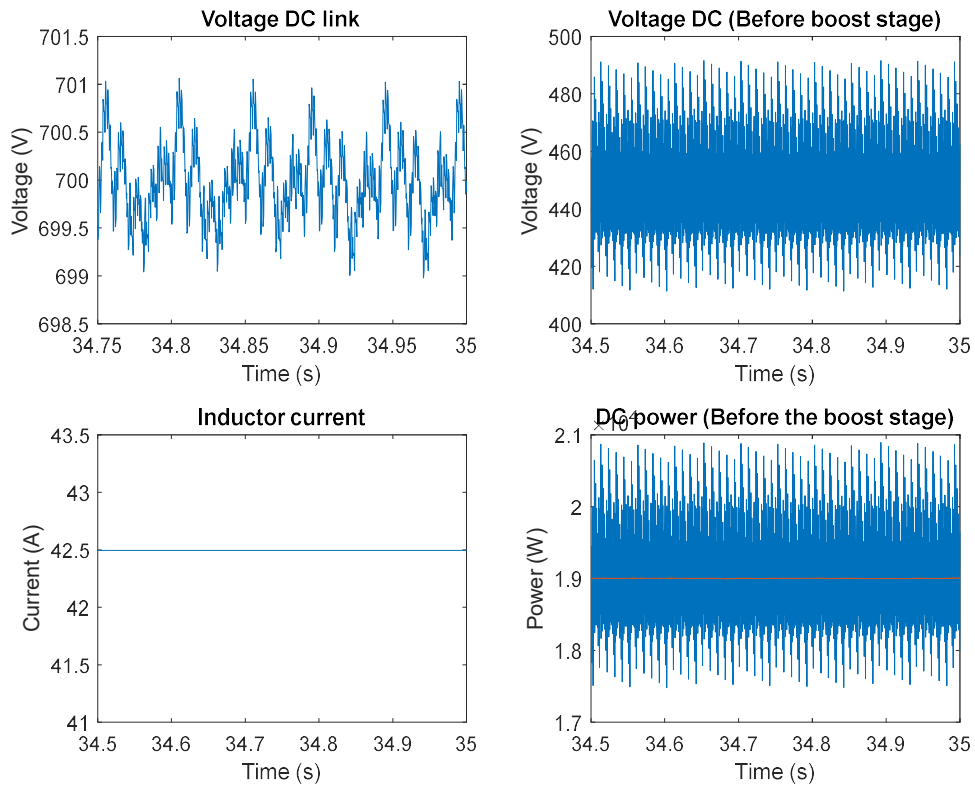


Figure 39: Steady-state average model DC link results.

As it can be seeing the real and the average system models, despite the second one loses some information the general behaviour is the same, and therefore for longer simulations in which the details are not so important it is preferable to use the average approach.

Looking at the electric side results from the model during steady-state, the system follows with the specifications for grid connection with a quite low THD and a close to 1 power factor, calculated from the currents during the dq rotating reference frame stage. This is in part possible given the great job that the boost stage does to stabilize the DC link voltage around 700 V with a margin of only around 1.2 %. Also, it gives a DC input link power close to the theoretical maximum of 20 kW.

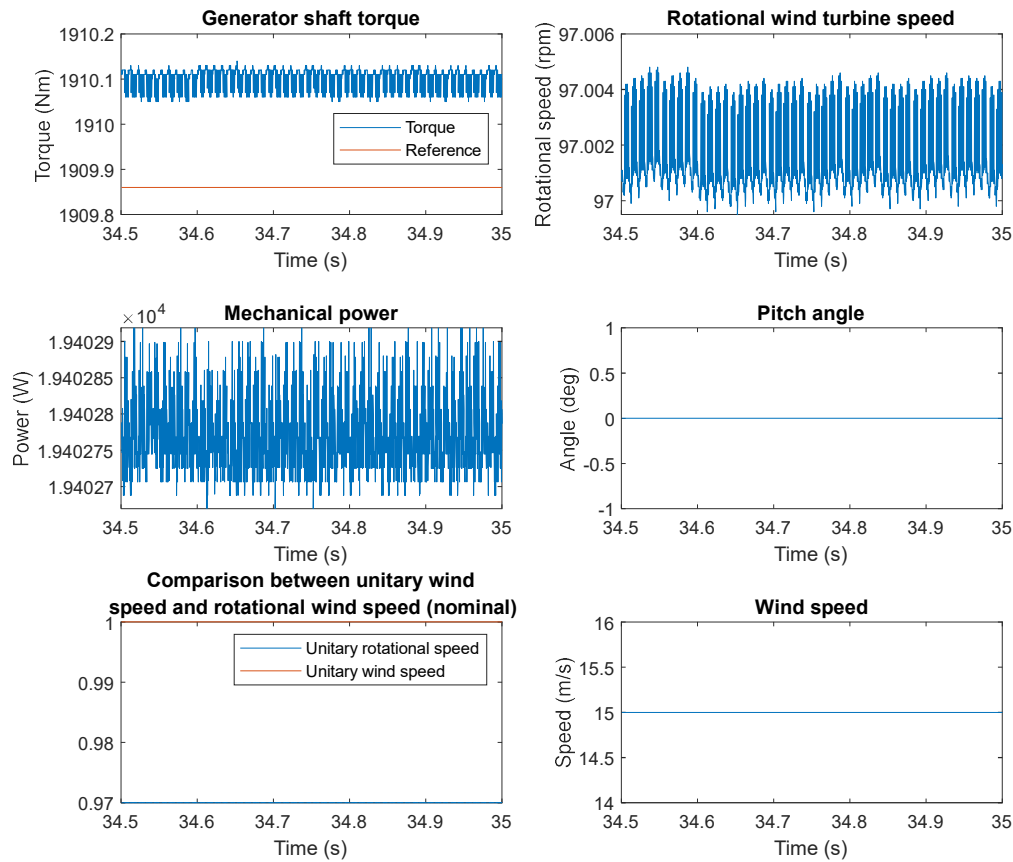


Figure 40: Steady-state average mechanical results.

The mechanical results, obtained from the average model shows a very stable and almost ripple free in some variables such as, the torque, the rotational speed of the wind turbine or the mechanical power. This simulation was done with a wind speed of 15 m/s (54 km/h), being this the nominal state for this particular turbine.

Transitory regime

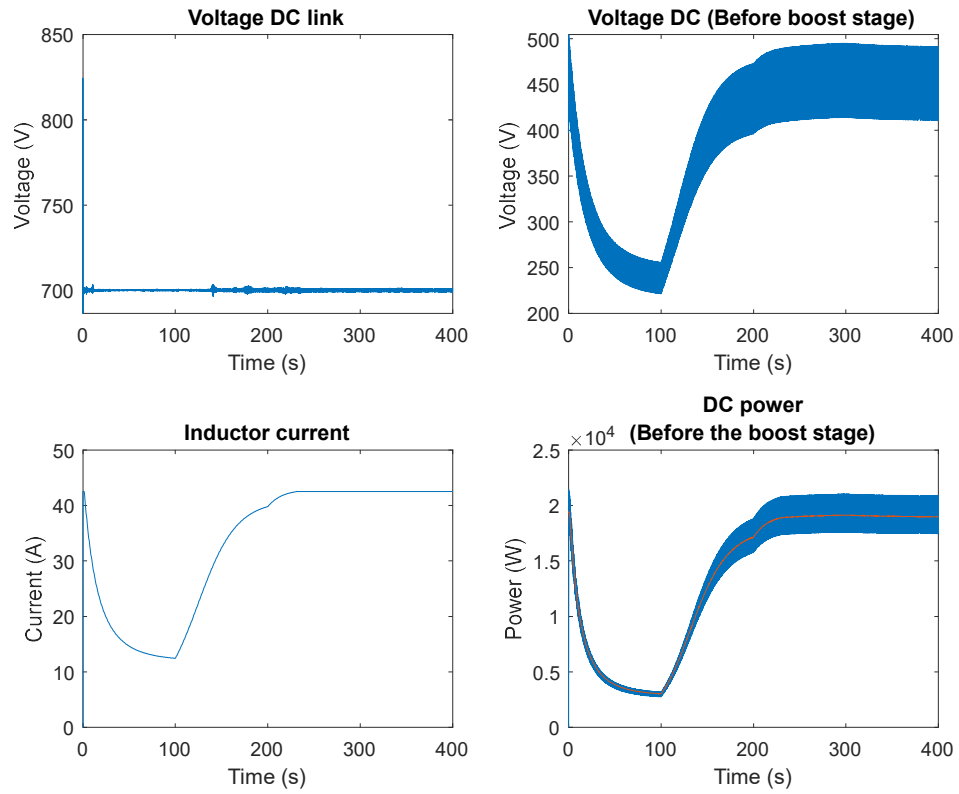


Figure 41: Transitory DC link results.

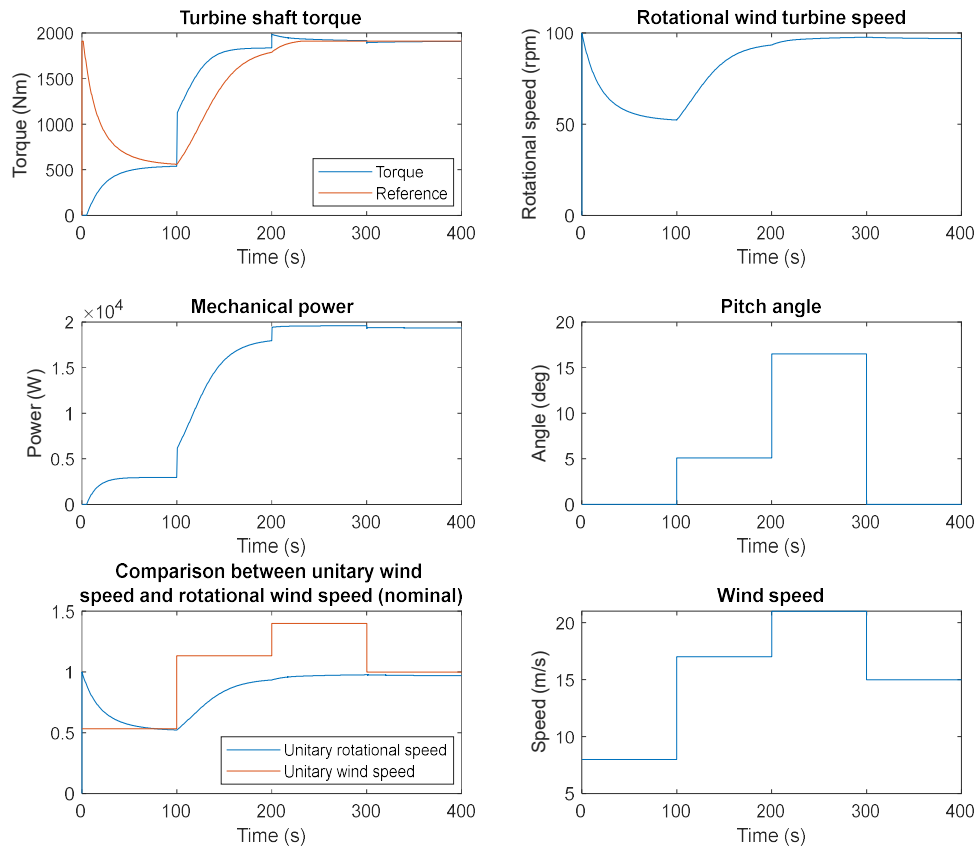


Figure 42: Transitory mechanical results.

During the transitory regime, caused by a changing wind speed, it is observed how at the beginning of the simulation (when the rotational speed is 100 rpm) the reference torque is a lot bigger than its final value for that particular wind speed and also how it follows in a certain way the rotational speed, showing that the reference torque is a function of the rotational speed. When the wind speed grows bigger than 15 m/s, which is the base nominal speed, the pitch control kicks in by limiting the power and therefore the rotational speed so the physical components of the system do not get damaged.

MPPT

Tip-speed ratio

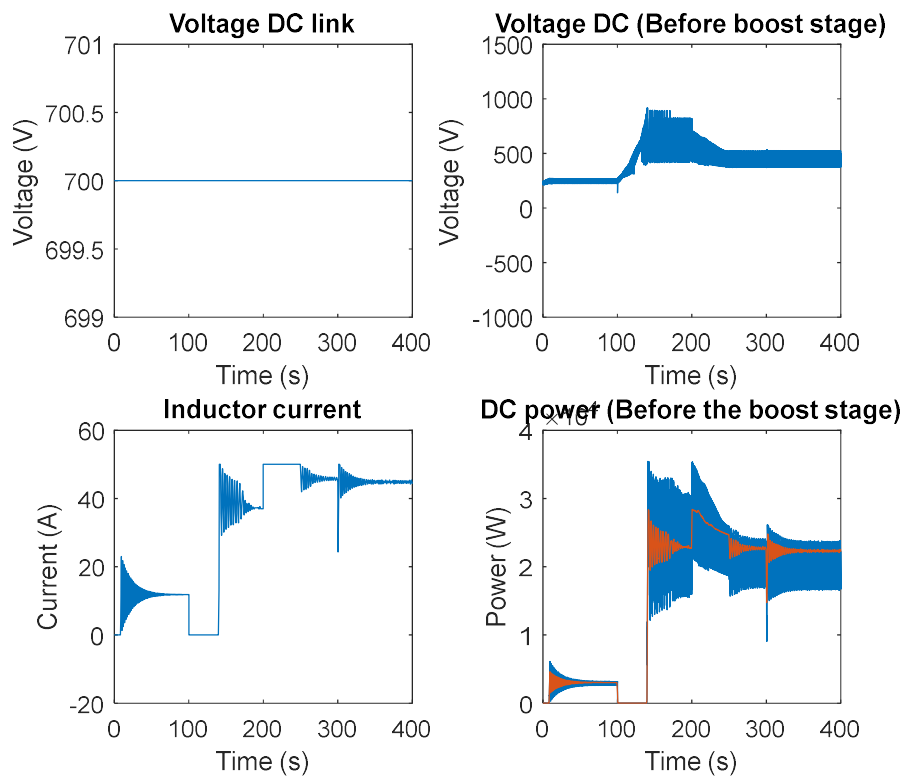


Figure 43: Transitory DC link results for TSR MPPT.

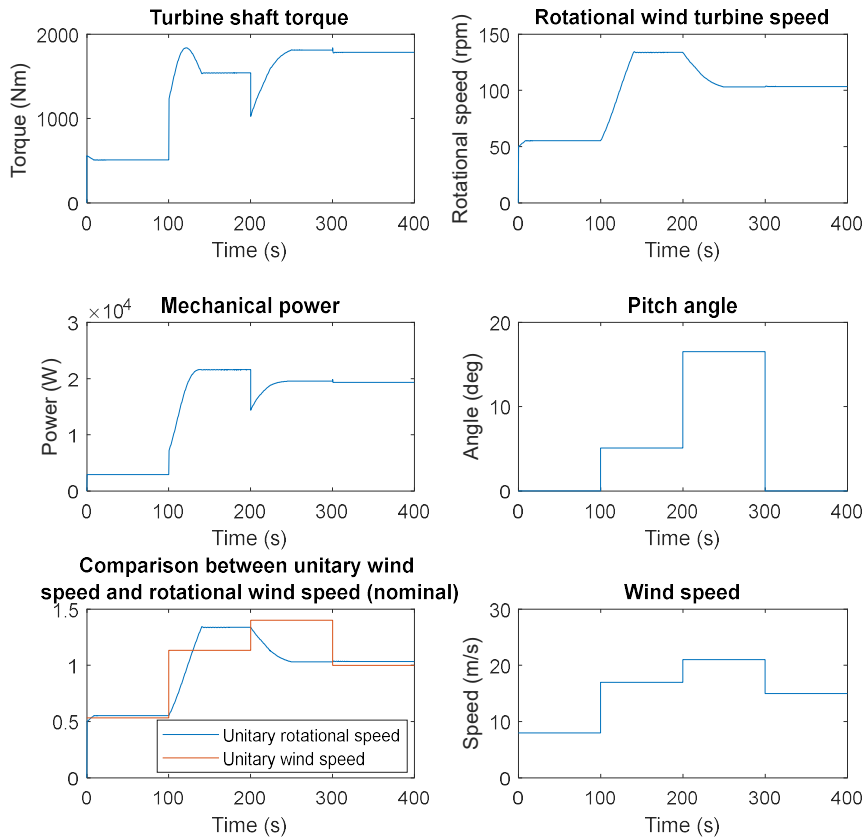


Figure 44: Transitory mechanical results for TSR MPPT.

Optimum torque

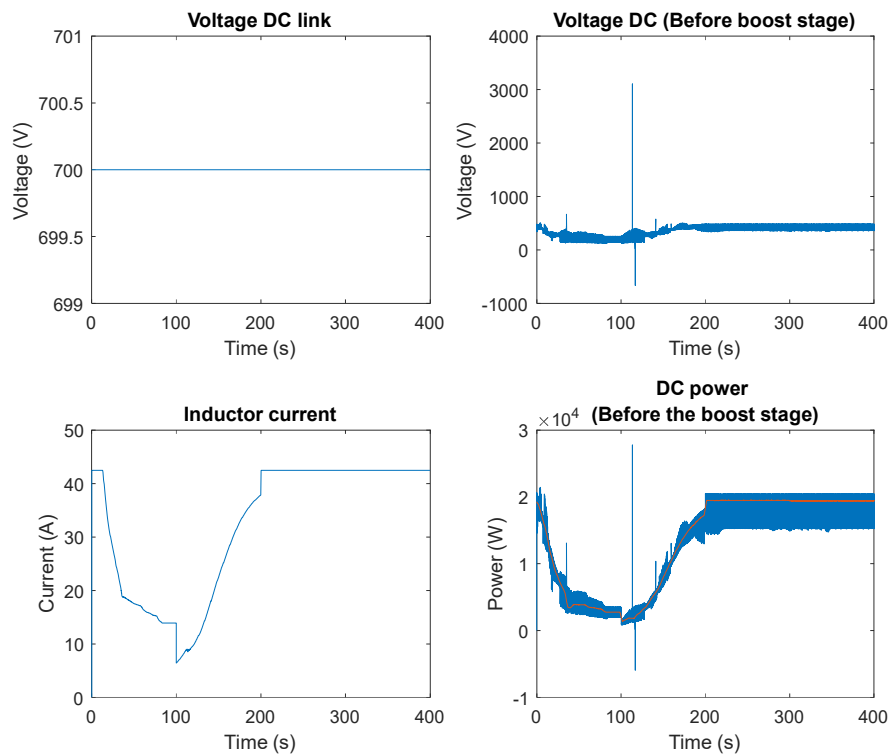


Figure 45: Transitory DC link results for OT MPPT.

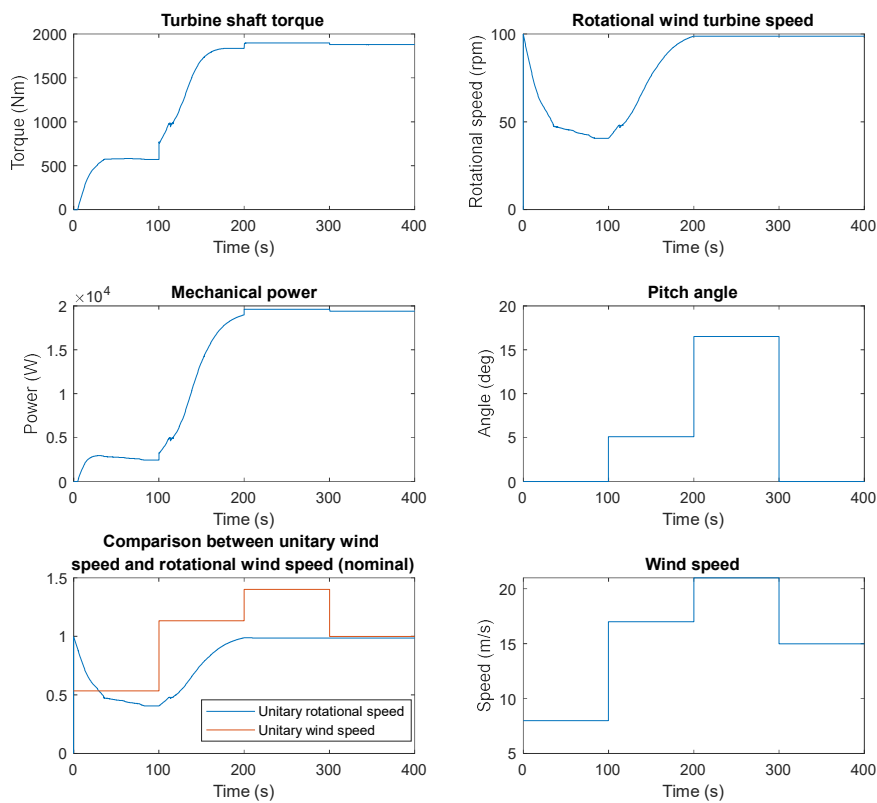


Figure 46: Transitory mechanical results for OT MPPT.

These results were generated by using the average model, but only the DC part, as the MPPT algorithms only modified this part of the model, that's why the voltage DC link is ideal. The approach used in this model doesn't include a torque sensor and instead uses electrical magnitudes, as it was exposed previously, that way there is no need for additional or costlier equipment, however the control strategy works perfectly for the intended application.

Power signal feedback

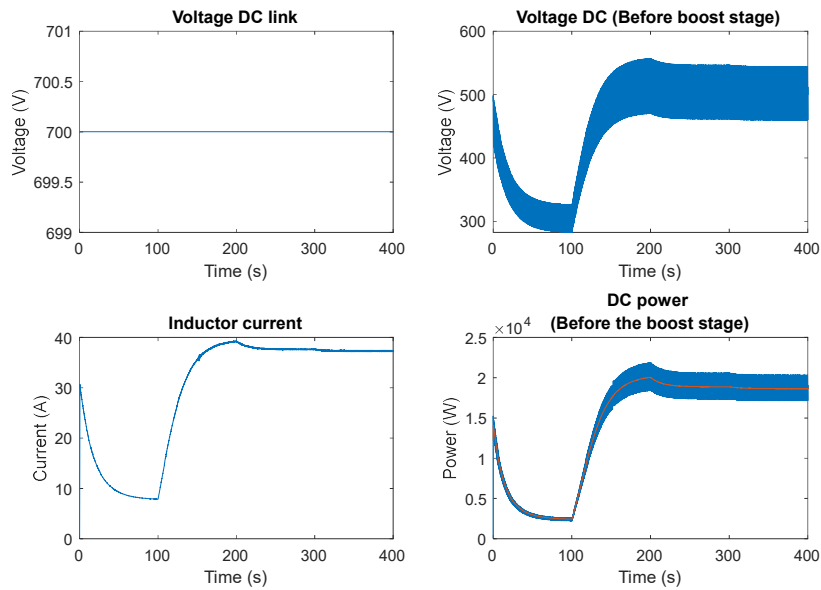


Figure 47::Transitory DC link results for PSF MPPT.

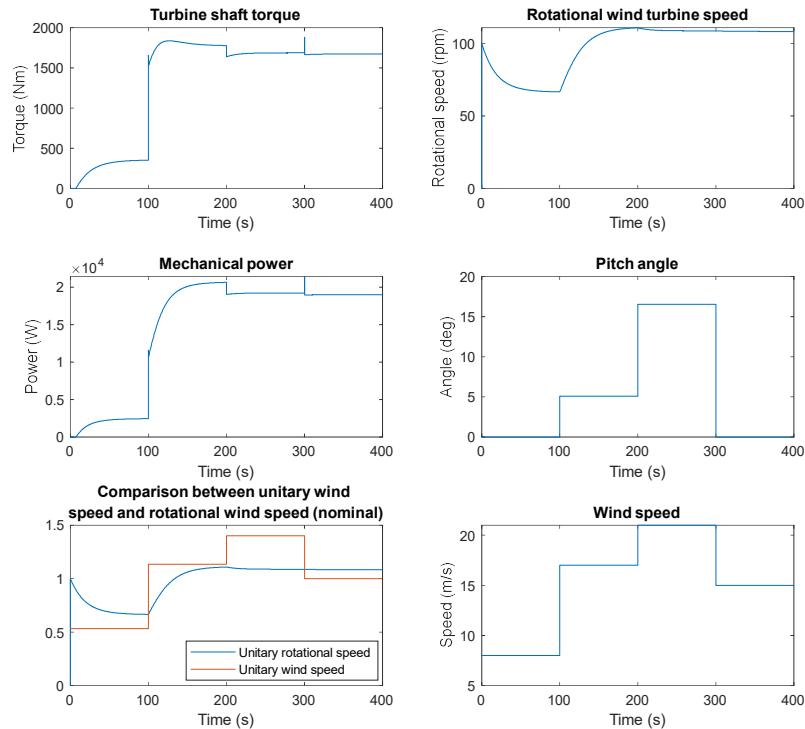


Figure 48:Transitory mechanical results for PSF MPPT.



In the end all three strategies works for this application, complexity wise are quite similar and their dynamic behaviour is almost identical with just a few punctual differences and to choose one over the other comes down to a criterion of what data is available for the controller and the particular situation.

Strategy	Fast enough	Additional sensors required	Complexity	Knowledge of the system required	Performance under varying wind conditions
Tip-Speed Ratio	Yes	Very precise wind speed.	Low	No	Adequate
Optimum torque	Yes	No, the measurement can come from electric magnitudes in certain cases.	Low	Yes	Adequate
Power signal feedback	Yes	No, the measurement can come from electric magnitudes, changing also the magnitude to control.	Low	Yes	Adequate
Perturb & observe	Too slow for most wind power applications	No	Low, on its basic form, with modifications can be very complex.	No	Too slow for the more unstable changes.

Conclusions

To conclude, the model behaves satisfactory as checks every requirement that was originally proposed for its creation, being an ideal system for relatively small power turbines, as all the generated power goes through the power electronics, for greater powers other strategies or more complex power electronics should be considered, such as parallelization of those.

This main disadvantage, enables certain characteristics that may be considered very attractive for some applications, it is a very simple system by comparison with alternatives, Double-fed generator, as the generation frequency has extensive margins, fact which allows for a better performance. Additionally, the dynamic response of the system is very quick, with both strategies, open or closed loop, which does not require additional sensors nor instantaneous information. For all of this it seems possible that only with minor modifications the model could be easily modified to accommodate, for example, multiple wind turbines (of a smaller power) tied together by the DC link.



References

- Asociación Empresarial Eólica. (2018). *Eólica 2018. La voz del sector*. Madrid.
- Abdullah, M. A., Yatim, A. H., Tan, C. W., & Saidur, R. (2012). A review of maximum power point tracking algorithms for wind energy systems. *Elsevier*, 3220-3226.
- Blanco Rubio, L. (2017). Diseño electromagnético de un motor síncrono de imanes permanentes para el accionamiento de la hélice de un barco. Madrid, España: Universidad politécnica de Madrid.
- Danish wind industry association. (23 de July de 2003). *WindDenmark*. Obtenido de <https://winddenmark.dk/>
- Erickson, R. W., & Maksimović, D. (2001). *Fundamentals of Power Electronics*. New York: Kluwer Academic Publishers.
- Heier, S. (2014). *GRID INTEGRATION OF WIND ENERGY ONSHORE AND OFFSHORE CONVERSION SYSTEMS*. Kassel, Germany: Wiley.
- Hussain, A., Sher, H. A., Murtaza, A. F., & Al-Haddad, K. (January de 2019). Improved Voltage Controlled Three Phase Voltage. *IEEE*.
- Kazmierkowski, M. P., Blaabjerg, F., & Krishnan, R. (2002). *Control in power electronics. Selected Problems*. London: Academic press. Elsevier science.
- Lastra, J. N. (2015). Modelado y control dinámico de un Aerogenerador. Santander.
- Lavín, S. Á. (June de 2015). Cottage household with wind power. Warsaw.
- M. A. Abdullah, A. H. (2011). A study of maximum power point tracking algorithms for wind energy system. *2011 IEEE Conference on Clean Energy and Technology (CET)* (págs. 321-326). Kuala Lumpur: IEEE.
- Manwell, J. F., McGowan, J. G., & Rogers, A. L. (2002). *Wind energy explained. Theory, design and aplication*. Amherst, USA: Wiley.
- N. M. Salgado-Herrera, F. M.-D.-R.-S. (2015). THD mitigation in type-4 Wind Turbine through AFE Back to back converter. *2015 North American Power Symposium (NAPS)* (págs. 1-6). Charlotte: IEEE.
- One Energy Enterprises LLC. (22 de 07 de 2020). *One Energy Enterprises LLC*. Obtenido de One Energy: <https://oneenergy.com/wind-knowledge/wind-turbine-information/>
- Oviedo-Salazar, J. M. (2015). Historia y Uso de Energías Renovables. *Daena: International Journal of Good Conscience*, 5-7.
- Pekarek, S. (8 de 11 de 1998). *IEEE*. Obtenido de <https://www.ewh.ieee.org/soc/es/Nov1998/08/BEGIN.HTM#INDEX>
- Powersim Inc. (2018). PSIM® User's Guide.



- S. M. R. Kazmi, H. G. (2010). Review and critical analysis of the research papers published till date on maximum power point tracking in wind energy conversion system. *IEEE Energy Conversion Congress and Exposition*, (págs. 4075-4082). Atlanta.
- Tunia, H., & Kazmierkowski, M. P. (1987). *Automatic control of converter-fed drives*. Warsaw: Elsevier.
- Wang, Q., & Chang, L. (2004). An intelligent maximum power extraction algorithm for inverter-based variable speed wind turbine systems. *IEEE Transactions on Power Electronics*, 1242-1249.
- WindEurope. (2019). *Wind energy in Europe*.

Annex 1: Table of illustrations.

Figure 1: Total power generation capacity in the European Union 2008-2018. Source: (WindEurope, 2019).	8
Figure 2: Percentage of the average annual electricity demand covered by wind. Source: (WindEurope, 2019).	9
Figure 3: Windmills, Campo de Criptana, Spain. Credit: Lourdes Cardenal.	10
Figure 4-. Charles F. Brush's turbine. Ohio, 1888.	10
Figure 5: Annual evolution and accumulated power in Spain. Green: Installed wind power (MW), Blue: Accumulated power. Source: (Asociación Empresarial Eólica, 2018).	11
Figure 6: Diagram graphically depicting parts of a wind turbine, including the tower, generator, nacelle, blade, hub, and rotor. Source: (One Energy Enterprises LLC, 2020)	13
Figure 7: General scheme of a wind power back to back conversion system. Source: (N. M. Salgado-Herrera, 2015)	14
Figure 8: Power coefficient in relation to the wind speed and rotational speed at different pitch angles ($R=12.5$ m, $\lambda=2$)	16
Figure 9: Power coefficient in relation to tip speed ratio for different pitch angles ($R=12.5$ m, $\lambda=2$)	16
Figure 10: Power characteristic at different wind speeds	17
Figure 11: Optimum characteristics of rotational speed vs. wind speed	17
Figure 12: Optimum characteristic of torque vs. wind speed	17
Figure 13: Optimum torque vs. optimum rotational speed	18
Figure 14: Schematic of the mechanical model	18
Figure 15: Small permanent magnet synchronous machine. Source: Water Fuel Energy Solutions.	19
Figure 16: Diagram of a PMSM. Source: The MathWorks, Inc.	21
Figure 17: Schematic of the wind turbine, generator, rectifier and boost converter.	22
Figure 18: Schematic of a Boost converter.	23
Figure 19: Transformation ratio of an ideal Boost converter.	23
Figure 20: Two average boost converter ideal commutation cell models resulting of the volt-second and capacitor charge balances.	24
Figure 21: Average boost converter ideal commutation cell model formed by two current dependant sources.	24
Figure 22: Average boost converter schematic.	24
Figure 23: Block diagram of the tip speed ratio control. Source: (M. A. Abdullah, 2011)	25
Figure 24: Block diagram of optimal torque control MPPT method. Source: (M. A. Abdullah, 2011)	26
Figure 25: block diagram of a wind energy with the power signal feedback control technique. Source: (M. A. Abdullah, 2011).	27
Figure 26: Line to line grid voltage in relation to the modulation ratio. $V_{DC}=350$ V, $f=60$ Hz. Source: (Kazmierkowski, Blaabjerg, & Krishnan, 2002)	29
Figure 27: Inverter and LCL filter schematic.	29
Figure 28: Inverter Voltage Oriented Control.	30
Figure 29: Calculation of theta angle for the abc to dq transformation.	30
Figure 30: Averaged inverter schematic.	31
Figure 31: Averaged inverter DC side controller.	31
Figure 32: Calculations for consumed power at the AC side.	31
Figure 33: Power factor calculation.	32
Figure 34: Complete schematic.	33
Figure 35: Complete schematic for the average model.	34
Figure 36: Steady-state "Grid-side" results.	35
Figure 37: Steady-state DC link results.	35
Figure 38: Steady-state average model "Grid side" results.	36
Figure 39: Steady-state average model DC link results.	36



Figure 40: Steady-state average mechanical results.	37
Figure 41: Transitory DC link results.	38
Figure 42: Transitory mechanical results.	38
Figure 43: Transitory DC link results for TSR MPPT.	39
Figure 44: Transitory mechanical results for TSR MPPT.	40
Figure 45: Transitory DC link results for OT MPPT.	41
Figure 46: Transitory mechanical results for OT MPPT.	41
Figure 47: Transitory DC link results for PSF MPPT.	42
Figure 48: Transitory mechanical results for PSF MPPT.	42
Figure 49: Example of abc to dq space transformation.	48
Figure 50: Example of abc to α - β space transformation.	49

Annex 2: Transformation and inverse transformation from *abc* to *dq* space.

The equation used to do the transformation from *abc* space to the *dq* space, with the q-axis leading the d-axis is:

$$\begin{bmatrix} v_d \\ v_q \\ v_0 \end{bmatrix} = \frac{2}{3} \cdot \begin{bmatrix} \cos(\theta) & \cos(\theta - \frac{2\pi}{3}) & \cos(\theta + \frac{2\pi}{3}) \\ -\sin(\theta) & -\sin(\theta - \frac{2\pi}{3}) & -\sin(\theta + \frac{2\pi}{3}) \\ \frac{1}{2} & \frac{1}{2} & \frac{1}{2} \end{bmatrix} \cdot \begin{bmatrix} v_a \\ v_b \\ v_c \end{bmatrix}$$

Where θ is the angle.

Being the inverse transformation:

$$\begin{bmatrix} v_a \\ v_b \\ v_c \end{bmatrix} = \begin{bmatrix} \cos(\theta) & -\sin(\theta) & 1 \\ \cos(\theta - \frac{2\pi}{3}) & -\sin(\theta - \frac{2\pi}{3}) & 1 \\ \cos(\theta + \frac{2\pi}{3}) & -\sin(\theta + \frac{2\pi}{3}) & 1 \end{bmatrix} \cdot \begin{bmatrix} v_d \\ v_q \\ v_0 \end{bmatrix}$$

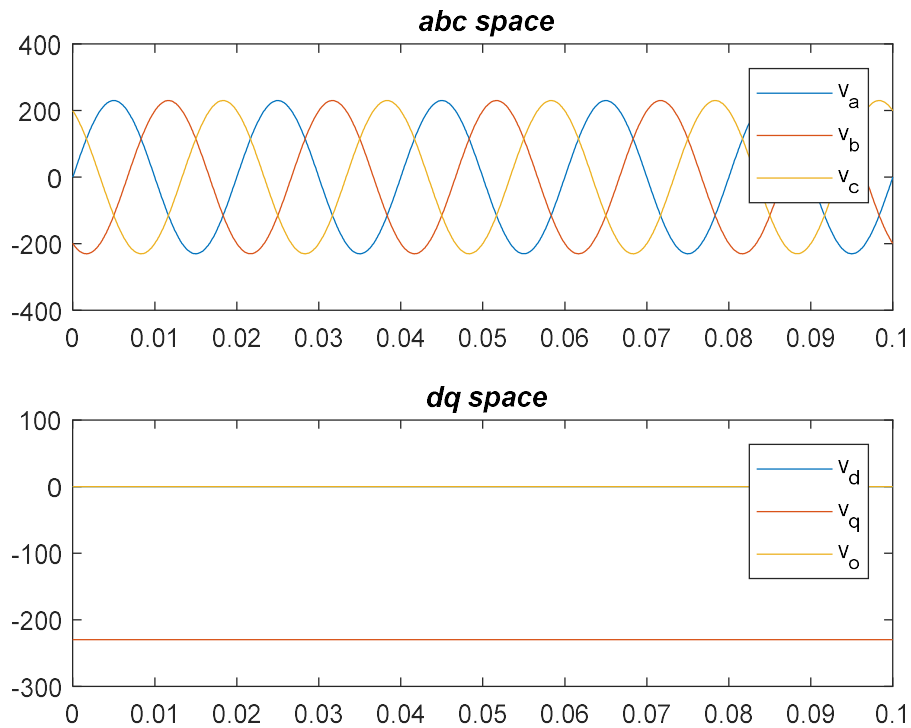


Figure 49: Example of *abc* to *dq* space transformation.

Annex 3: Transformation from *abc* to *alpha-beta* ($\alpha\beta$) space.

The transformation used is based on the amplitude invariant:

$$\begin{bmatrix} v_\alpha \\ v_\beta \end{bmatrix} = \frac{2}{3} \cdot \begin{bmatrix} 1 & -\frac{1}{2} & -\frac{1}{2} \\ 0 & \frac{\sqrt{3}}{2} & -\frac{\sqrt{3}}{2} \end{bmatrix} \cdot \begin{bmatrix} v_a \\ v_b \\ v_c \end{bmatrix}$$

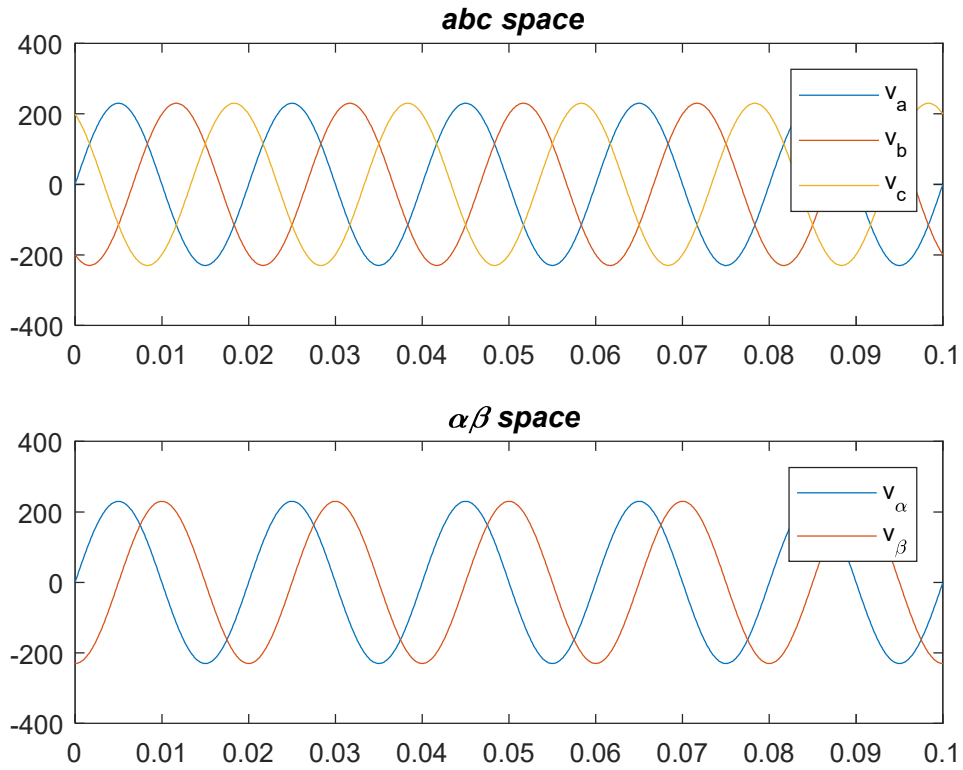


Figure 50: Example of *abc* to *alpha-beta* space transformation.